Review

pubs.acs.org/Biomac

Multivalent Polymers for Drug Delivery and Imaging: The Challenges of Conjugation

Mallory A. van Dongen, Casey A. Dougherty, and Mark M. Banaszak Holl*

Chemistry Department, University of Michigan, Ann Arbor, Michigan 48103, United States

ABSTRACT: Multivalent polymers offer a powerful opportunity to develop theranostic materials on the size scale of proteins that can provide targeting, imaging, and therapeutic functionality. Achieving this goal requires the presence of multiple targeting molecules, dyes, and/or drugs on the polymer scaffold. This critical review examines the synthetic, analytical, and functional challenges associated with the heterogeneity introduced by conjugation reactions as well as polymer scaffold design. First, approaches to making multivalent polymer conjugations are discussed followed by an analysis of materials that have shown particular promise biologically. Challenges in characterizing the mixed ligand distributions and the impact of these distributions on biological applications are then discussed. Where possible, molecular-level interpretations are provided for the structures that give rise to the functional ligand and molecular weight distributions present in the polymer scaffolds. Lastly, recent strategies employed for overcoming or minimizing the presence of ligand distributions are discussed. This review focuses on multivalent polymer scaffolds where average stoichiometry and/or the distribution of products have been characterized by at least one experimental technique. Key illustrative examples are provided for scaffolds that have been carried forward to *in vitro* and *in vivo* testing with significant biological results.

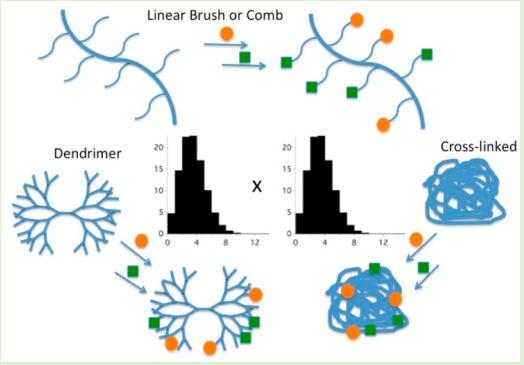

THE PROMISE OF MULTIFUNCTIONAL POLYMER SCAFFOLDS FOR THERAPEUTICS AND DIAGNOSTICS

Conjugation of polymer scaffolds with multiple copies of targeting ligands, drugs, and dyes has become a popular approach for achieving the aim of theranostics: materials useful for both diagnosis and treatment of disease (Figure 1).[1−9]

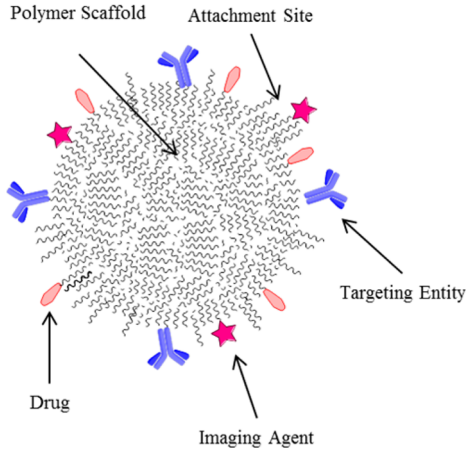

Figure 1. Theranostic consisting of targeting agents, drugs, and imaging agents on a polymer scaffold with many attachment sites, which may be at the terminal ends of the polymer or spread within the polymer backbone.

Enhanced targeting via multivalent binding, reporting location of action, and optimal impact at the target via delivery of a multidrug payload are important goals of theranostic design. In this manner, researchers hope to speed diagnosis and treatment as well as improve a drug's therapeutic index.[5,10−12] These concepts were summarized in 1975 by Ringsdorf, who noted that polymer conjugates offer the possibility to continuously vary active size and functionality on the scaffold and therefore tune solubility, toxicity, and biodistribution.[13] However, this flexibility in terms of property design introduces an inherent challenge common to theranostics as well as multivalent polymers designed solely for targeting, imaging, or therapy: heterogeneity introduced by the attachment of functional ligands to polymer scaffolds.[14,15]

This critical review will first address the source of conjugation heterogeneity and provide examples of how such heterogeneity is encountered and treated in the literature. We will then discuss how heterogeneity can impact the function of multivalent polymers and theranostics. Finally, we will review recent approaches to overcoming conjugation heterogeneity. Scaffold heterogeneity (i.e., polydispersity of the polymer) is also an important consideration for developing well-defined, clinically relevant polymer therapeutics. Scaffold polydispersity is dependent on both the chemical nature of the polymer and the backbone structure (linear, branched, hyperbranched,

Received: June 23, 2014
Revised: August 6, 2014
Published: August 14, 2014

   dx.doi.org/10.1021/bm500921q | *Biomacromolecules* 2014, 15, 3215−3234

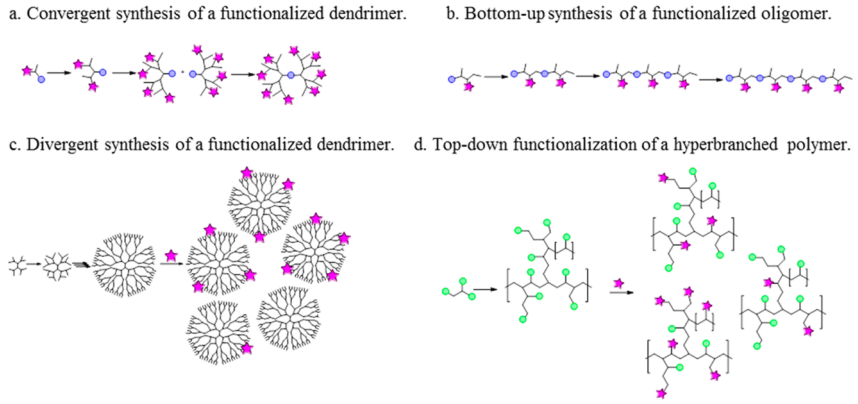

Figure 2. Schematic representation of the approaches to multivalent polymer conjugations. (a) Convergent synthesis of dendrimers allows for precise control but limited valency and size. (b) Bottom-up synthesis of conjugates allows for precise variation of regiochemistry but is confined to oligomers. (c) Divergent synthesis of dendrimers and (d) linear comb or hyperbranched polymers allow for larger polymers but generate random valency statistics.

dendritic). The effect of polydispersity from polymer synthesis strategies (i.e., bottom-up/divergent and top-down/convergent approaches) on resulting conjugates will also be addressed. For readers interested in the implications of ligand conjugation distributions and the resulting distribution of physicochemical, functional, and biolocalization properties upon United States Food and Drug Administration (U.S. FDA) and European Medicines Agency (EMA) approval of medicinal, drug, cosmetic, and food products, we refer to the recent book *Characterization of Nanoparticles Intended for Drug Delivery* prepared by the Nanotechnology Characterization Laboratory of the National Cancer Institute and recent reviews on the subject.[16−21]

As we will examine in detail, the material resulting from the various synthetic strategies differs in terms of final polymer structure. The ideal convergent polymer synthesis strategy can result in nearly molecular control of structure with full control of three-dimensional architecture, molecular weight, and hydrophobicity. From the point of view of making reproducible material and achieving uniform biodistribution and pharmacokinetics, these are highly desirable properties. However, challenges to the convergent strategy include scaling syntheses to production levels and achieving materials in higher molecular weight ranges. A less obvious concern is that following this strategy to make a single material with a particular set of toxicity, imaging, biodistribution, and pharmacokinetics properties is akin to performing small molecule drug discovery one molecule at time, a practice that has long since given way to the evaluation of libraries of lead compounds. At this time, little data exists for most polymer systems, with the exception of monofunctional poly(ethylene glycol) (PEG),[22−25] to predetermine the ideal ligand-to-scaffold ratios for synthetic efforts. Synthetic strategies employing preformed polymer scaffolds offer the promise of a greater range of molecular weights and cheaper, more readily scalable scaffold syntheses. Challenges to such approaches include molecular weight dispersity in the scaffold and statistical distributions of conjugated, functional ligands that can yield mixtures of tens, hundreds, or thousands of structures, with the accompanying variation in toxicity, imaging, biodistribution, and pharmacokinetic properties. The ability to reproduce such mixtures at production scale is also a grave concern. However, if one ceases to tout the homogeneity of such materials and instead embraces the library of important properties generated, then these methods provide an interesting way to screen activity of a wide array of ligand-to-scaffold ratios, and even molecular weights, which may lead to the desired biological properties. In addition, given the heterogeneous properties of some diseases, such as cancer, a range of properties may be desirable. Applying such mixtures of materials to discovery of new biomedical applications is, in this sense, akin to current small molecule library strategies. However, testing these mixtures leaves the researcher with the difficult task of identifying which fractions are responsible for beneficial properties. This approach has been most fully explored to date in the development of BIND-014, a poly(D,L-lactide) (PLA) and PEG copolymer encapsulating docetaxel that is targeted via prostate-specific membrane antigen (PSMA).[26,27] The general strategy of self-assembly of functionalized components,[5] a convergent approach, has also been exploited for siRNA treatment of solid tumors (CALLA-01)[19] and for a nicotine vaccine (SEL-068).[19,28] The BIND, CALLA, and SEL systems will not be discussed further, as they are noncovalent self-assemblies subject to substantially different kinetic and thermodynamic challenges in terms of assembly, biological stability, and ligand distributions compared to those of the covalent polymer scaffolds that are the focus of this review.

Attachment of multiple targeting ligands enhances binding of the polymer conjugate to cells and tissues that overexpress a certain receptor.[2,7,23,29,30] Active targeting can minimize negative side effects in healthy tissues and allow for a higher tolerable dosage of drug. High loading of molecular drugs, such as chemotherapeutics like methotrexate[31] or antibiotics like vancomycin,[32] onto the polymeric scaffold[7,29,30] enables multivalent delivery of the drug to the same cell. Conjugation of fluorescent dyes to polymers, to allow for *in vitro* and *in vivo* imaging, solubilizes the typically hydrophobic dyes and enables imaging of biological structures and studies of conjugate biodistribution. When creating theranostics, two[33−36] or three[37−40] subsequent multivalent modifications are performed on the same scaffold to create a multifunctional, targeted, drug delivery vehicle that can be tracked by fluorescence microscopy.

APPROACHES TO FORMING MULTIVALENT POLYMER CONJUGATES

The polymer conjugate can be formed by (I) assembly of functionalized components concomitant with the formation of the polymer backbone or (II) reaction after the polymer

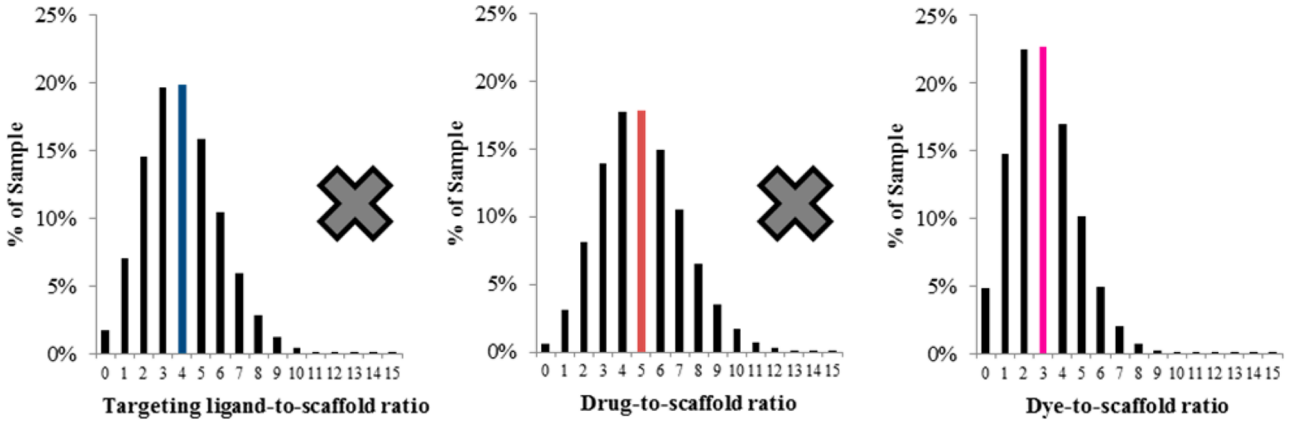

Figure 3. Distributions resulting from stochastic conjugations with an average of 4, 5, and 3 ligands have a cumulative, multiplicative effect on sample heterogeneity. With each subsequent serial conjugation, the resulting set of products is the product of the resulting Poisson distributions. For each case, the mean of the distribution is illustrated with a colored bar.

scaffold has been assembled. Process I is illustrated as a convergent dendrimer synthesis (Figure 2a)[41−44] and as polymerization of functional oligomers (Figure 2b) employing units to which the desired targeting agent, drug, or dye is already attached. In process II, the functional group is attached after the scaffold is formed, and this is illustrated for materials synthesized using a divergent dendrimer synthesis (Figure 2c)[45−54] and for hyperbranched polymers (Figure 2d).

For purposes of controlling conjugation and scaffold heterogeneity, convergent strategies offer many advantages.[55−57] Dendrimer made in this fashion tends to have fewer missing branches, and synthetic procedures can generally be carried out with stoichiometric amounts of reagents, as opposed to the vast excesses frequently necessary for divergent syntheses. If the convergent process originates from the functional ligand, heterogeneity of the conjugated functional group in the final product is directly correlated with scaffold defects and, for lower-generation dendrimers at least, can be quite low. The two major limitations on this strategy include efficiently achieving the central coupling step as generation increases and the requirement that the number of functional groups is a multiple of the number of arms (Figure 2a). The difficulty in completing the central coupling step as generation increases results in an overall limitation on polymer size and molecular weight. Strategies to get around this problem have included a hybrid approach that employs both divergent and convergent strategies;[58] however, this does induce heterogeneity of the kind discussed in the next section. The nondendrimer equivalent to a convergent approach would be bottom-up synthesis of oligomer scaffolds to include multiple copies of the ligand of interest or attachment sites within the oligomer backbone (Figure 2b). For example, sequence-specific incorporation of a click ligand onto a peptoid backbone.[59] This procedure is also limited by the cost of synthesis and is limited to only shorter oligomers with molecular control.

Conjugation of ligands to preformed polymer scaffolds is generally accomplished by one-pot or sequential attachment of the ligands to generate the desired average ligand-to-scaffold ratio (Figure 2c,d). This typically allows for larger scale syntheses of the polymer scaffold (i.e., divergent synthesis of dendrimer and traditional polymerization techniques for other architectures). The polymer scaffold often has many sites available for chemical modification; for example, poly(amidoamine) (PAMAM) dendrimers have (theoretically) 4−4000 primary amines, depending on generation (G1−G11), available for peptide coupling.[60,61] For nondendritic scaffolds, the number of attachment sites varies by formulation chemistry of the monomer, architecture (branched, linear), molecular weight, and scaffold polydispersity/molecular weight distribution. Such scaffolds have the advantage of many possible conjugations sites and high MW, enabling them to provide solubility to many hydrophobic ligands; however, conjugation results in a statistical distribution of ligand-to-scaffold ratios.[14,15]

Examples of the impact of conjugation statistics on product distributions are discussed below. Additional useful discussion of this problem can found be in a number of recent articles and reviews.[14,15,62−64] Consider a generic case where a multivalent polymer scaffold with a large excess of attachment sites is conjugated to an average of 4 targeting ligands, 5 copies of a drug, and 3 molecular dyes. Such a theranostic is commonly represented in the literature by a cartoon such as that in Figure 1. The statistically controlled reaction between each ligand and the available scaffold sites generates a Poisson distribution of products (Figure 3). The attachment of 4 targeting agents to the scaffold results in 14 unique species with ligand-to-scaffold ratios ranging from 0 to 13. Although the dendrimer conjugated to 4 targeting agents is the most common species in this distribution, it represents only approximately one in five (20%) species present in the sample. To further complicate matters, heterogeneity due to stochastic conjugation is multiplicative. When the targeted scaffold is further treated with 5 equiv of drug, a new distribution is created. Approximately 15 drug-to-scaffold ratios are present in this new sample, with approximately 9 in 50 (18%) particles having 5 copies of the drug per scaffold. However, there are now over 200 unique species present in the sample resulting from the product of the first two Poisson distributions. After adding a third entity (3 equiv of dye), there are now approximately 2500 unique ligand-to-scaffold ratios present in the sample. The single entity pictured in Figure 1 illustrates the arithmetic mean of each individual distribution (i.e., 4 targeting agents, 5 drugs, 3 dyes), but it represents just 1 out of every 250 (0.8%) particles present. Although it is the "average" material present, this average may not be meaningful in terms of biological behavior for any of the desired functional behaviors: targeting, therapeutic effects, or imaging. For any observed function of this material, whether in cell culture or *in vivo*, the challenge of

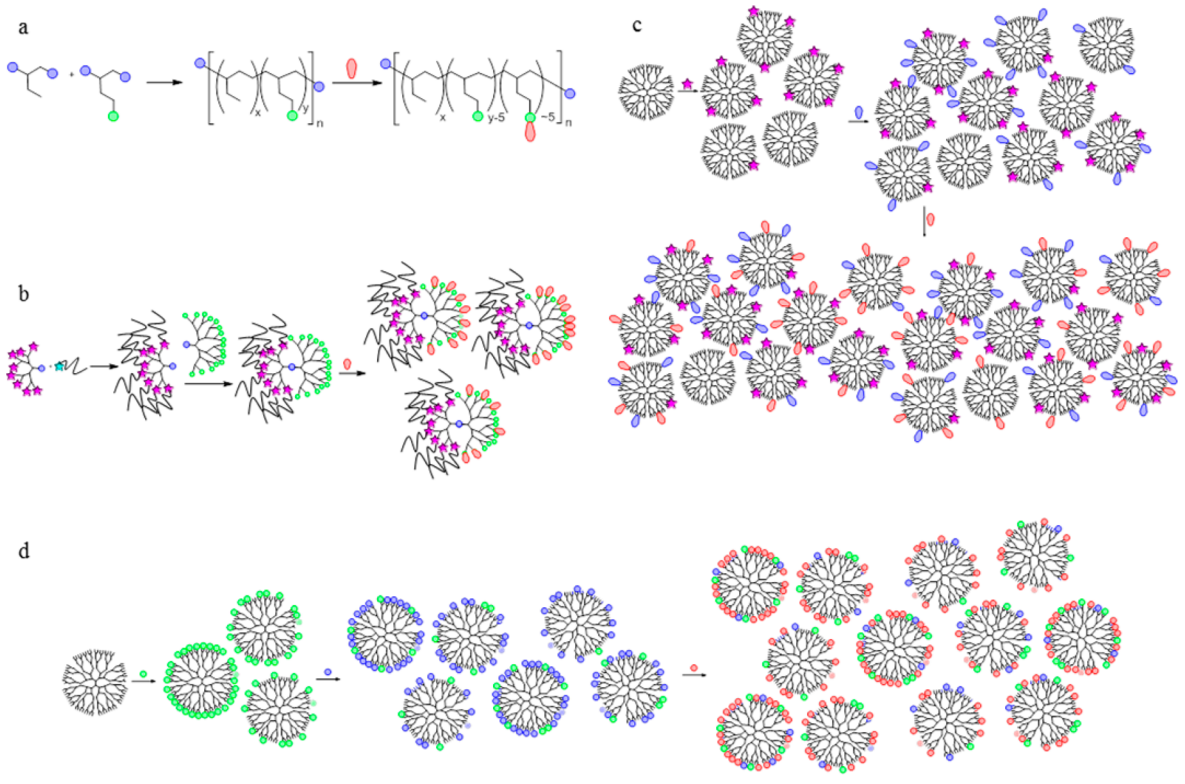

Figure 4. Schematic illustration of the synthesis strategy and product distribution for (a) Kopeček's comb polymer PK1,[69] (b) Szoka and Fréchet's bow-tie dendrimer,[75] (c) Baker's PAMAM-FITC-FA-MTX conjugate,[9,76,77] and (d) Kannan's PAMAM-NAC conjugate.[78]

understanding which fraction(s) of the 2500 species provide the desired activity raises a major hurdle to translating exciting results to the clinic.

The inherent challenges represented by these distributions can be further explored by considering additional quantitative aspects. Two percent of the sample lacks any targeting ligand and thus biodistribution is controlled primarily by size and hydrophobicity considerations. In addition, 9% of the sample contains less than two target ligands, which rules out any multivalent targeting for this fraction of the sample. One out of every 25 (4%) particles has fewer than 2 drugs attached and no longer has potential for increased activity compared to that of the free drug. One particle in 20 (5%) has no dye on it and is invisible to the intended imaging modality. One particle in 20 also has twice the amount of expected dye, and 1 in 100 (1%) particles has three times the average amount of dye. Indeed, the roughly 10 different dye/polymer ratios per particle result in dramatically different local concentrations of dye. This difference is greatest between 1 and 2 dye/particle, where there is an approximately 7 orders of magnitude difference in local concentration for a ∼30 kDa polymer. This causes dramatic changes in absorption and emission properties (*vide infra*).[65,66] The preceding analysis has not yet considered the heterogeneity of the sample resulting from the polymeric scaffold, which can vary greatly, or spatial and regioisomers of multiple ligands, which can further impact the system. For polymer systems containing substantially restricted motion of the surface groups (i.e., cross-linked polymers, dendrimers with surfaces at the de Gennes packing limit, self-assembled systems when particles are gelled or solid, and all classes of inorganic nanoparticles), spatial isomers can rapidly lead to tens of thousands of functionally different isomers from a targeting, and possibly therapeutic, standpoint for the simple example illustrated in Figure 1. In addition to the 2500+ species present from statistical considerations, the molecular weight dispersion present in even relatively homogeneous polymers will lead to different biodistribution behavior. For example, although polymers in the 20−30 kDa range are expected to be excreted through the kidney, polymers of 60−100 kDa are expected to be trafficked to the liver.[46,67] The full statistical range of ligand conjugation convoluted with each mass range generates further challenges for understanding the origin(s) of both positive, desired effects as well as origin(s) of negative side effects. In addition, such complex mixtures offer a substantial challenge for reproducible synthesis when scaling the material from the milligrams needed for exploratory work to the kilograms required for clinical trials and drug productions.

SELECT EXAMPLES OF CONJUGATION HETEROGENEITY IN THE LITERATURE

The theoretical conjugation described above is representative of serial conjugations often encountered in the literature. For such materials, mean conjugation numbers are often assumed from initial stoichiometry of reactants, and explicit analyses to determine experimental average conjugation numbers are often not reported. For translation of a theranostic to the clinic, experimental measurement of average stoichiometry will likely be a minimal expectation, with an even more detailed understanding of product mixture likely necessary. For the purpose of this review, we will focus on multivalent materials where average stoichiometry and/or the distribution of products have been characterized by at least one experimental technique. In addition, the illustrative examples in this section are chosen because they have been carried forward to *in vitro* and *in vivo* testing with significant biological results.

The first clinically investigated polymer−drug conjugate developed for cancer therapy, the comb polymer PK1, developed by Kopeček, Duncan, and others, consists of a linear *N*-(2-hydroxypropyl)methylacrylamide (HPMA) chain functionalized with a degradable Gly-Phe-Leu-Gly linker containing a terminal doxorubicin.[68−71] The material used in phase I and II clinical trials was 30 kDa and contained 8.5 wt % doxorubicin, corresponding to an average of 5 drugs per 13 available degradable linker sites on each polymer chain (Figure 4a). Assuming a stochastic conjugation, approximately 1 in 5 chains (20%) contained 5 drugs and about 1 in 10 chains (10%) contained 3 drugs in the full distribution from 0 to about 10 drugs per polymer chain. The actual distribution is likely substantially broader, since this estimate does not include the distribution in available linker sites per chain or the MW dispersity in chain size. The combination of these effects gives rise to tens to hundreds of species with variation in chain, hydrophobicity, and size that will give a range of distribution and pharmacokinetic properties. Efforts to improve MW dispersity of HPMA have included the development of atom transfer radical polymerization (ATRP) and reversible addition−fragmentation chain transfer (RAFT) polymerization.[72,73] The comb polymer approach has also been employed for acetylene-functionalized poly(lactide) polymers combined with click functionalization using PEG and paclitaxel.[74] Another approach has been to avoid size dispersity inherent to linear polymers by moving to dendritic polymer architectures.

The bow-tie dendrimer developed by Fréchet and Szoka combined a G3 polyester dendron terminated with poly(ethyleneoxide) (PEO) chains with a G4 polyester ester dendron linked to doxorubicin.[75] This material was particularly exciting because a single dose effectively treated C26 colon carcinoma xenograft tumors in mice. The 8−10 wt % drug loading based on absorbance measurements corresponds to an average of about 5−7 doxorubicin molecules per 16 arm G4 dendron (Figure 4b). The two-step synthetic process used a vast excess of linker agent. Presuming complete reaction at this step, an average of 6 doxorubicin ligands would be present on 1 in 5 (20%) of the bow-tie dendrons, with a Poisson distribution giving about 9 ligand-to-scaffold ratios. Alternatively, for this example, in which the doxorubicin is conjugated onto 16 locations on one dendron arm, it is possible that steric constraints limit the number of doxorubicin bound per scaffold and served to narrow the distribution; however, ensemble-level characterization did not allow the two structural alternatives to be distinguished.

The Baker group has extensively used G5 PAMAM dendrimer coupled with stochastic conjugation of targeting, imaging, and therapeutic ligands.[9,76,77] The theranostic covalently conjugated to 5 dyes (FITC), 5 targeting ligands (folic acid), and 5 methotrexates, which showed exceptionally promising *in vitro* and *in vivo* activity, is one of the more complex materials.[31] The three stepwise conjugations of targeting agent, drug, and dye to G5 PAMAM (M_N ∼28 kDa, PDI ∼1.1, with ∼110 amine end groups) result in over 4000 unique combinations (Figure 4c). Only 1 particle in 200 (0.5% of the sample) has 5 copies of each ligand and corresponds to the arithmetic mean. Additionally, both folic acid and methotrexate have two carboxylic acids that can react with the amines of the scaffold (with one isomer being more active than the other), leading to as many as 14 400 possible combinations if folic acid regioselectivity is taken into account. Despite the complexity of the mixture, this material was capable of completely eliminating KB xenograft tumors in mice.

Another important example of stochastic conjugation was recently reported by Kannan, Romero, and Kannan using G4 PAMAM dendrimers developed for treatment of cerebral palsey.[78] An initial stochastic conjugation of Boc-GABA (GABA = γ-aminobutyric acid) provided a conjugate with an average of 30 GABA ligands per 64 theoretical surface sites, thus generating an approximate Poisson distribution ranging from about 20−40 GABA ligands per dendrimer. The active agent, *N*-acetyl-L-cysteine (NAC), was then attached via the GABA ligands using two additional conjugations steps, each going to about 80% completion (Figure 4d). The resulting material had an average ligand-to-scaffold ratio of 20 NAC ligands according to NMR and MALDI-TOF MS measurements. The initial GABA conjugation enforces the mean number of about 20 NAC ligands per dendrimer to be less than 10% of the total mixture with greater than 20 species present. Importantly, this mixture successfully reversed the symptoms of cerebral palsy in a rabbit disease model.

These four examples illustrate the promise of multivalent polymer conjugates as well as the challenges. In each case, the active, therapeutic fraction(s) are yet to be identified. In addition, the fraction(s) that contribute to toxicity remain to be identified. Viewed from this perspective, much work remains to optimize the therapeutic impact of such systems. Although multiple monovalent poly(ethylene glycol) (PEG) conjugates are in the clinic,[2,5,23,26] multivalent polymers have proven to be more difficult to translate. PK1 failed in phase II clinical trials. The Baker group was unable to scale the active components in their mixture to the kilograms needed to proceed to phase I clinical trials. Unfortunately, the scale-up process, which is expected to be difficult for the complex mixtures, generated material that was chemically and biologically inconsistent.[79] Still, in all four cases, a highly active fraction of material appears to be present. The problem is analogous to a therapeutic natural product present in a few percent in the bark of a tree, a microbe in the ground, or the mold on a crust of bread. The community needs to identify the active substances present in such polymer−conjugate mixtures, isolate them in a purer form, and test their efficacy.

Upon examination of ligand distribution challenges associated with the linear HPMA polymer (PK1), PAMAM dendrimer, and poly(ester) dendrimer scaffolds, the distribution of species resulting from statistically controlled reactions can appear daunting. This is particularly true for dendrimer systems where knowledge of both molecular weight and the mean number of multiple ligands present on the well-defined scaffold allows for a detailed analysis of the full range of products. It is important to realize that the lessons from the dendrimer analysis apply to all polymer scaffolds onto which a series of ligands is conjugated. In fact, the distributions and number of species estimated for the dendrimer systems serve as a lower bound because most other polymer scaffolds will have a greater MW distribution.

We conclude this section by examining G4 poly-L-lysine (PLL) dendrimer with napththalene disulfonic acid conjugated to the surface (SPL7013), which has been developed by Starpharma as VivaGel. This material has undergone nine clinical trials, including multiple phase III studies, and it is currently in a phase III clinical trial for use as a topical microbicide for bacterial vaginosis.[80−82] In this case, the base polymer has a MW of 4157 Da with roughly 90% of the sample

corresponding to the theoretically expected structure based on MALDI-TOF MS and high-performance liquid chromatography (HPLC) analysis.[80] Conjugation of the 16 surface amines yielded material with a MW of 14 020 Da, the theoretically expected value, with a range of other material between ~1342 and 14 630 Da. In this instance, the Poisson distributions present in the previous four examples were avoided by the exhaustive conversion of all surface amines with conjugated ligand. HPLC analysis suggests that 95% of the product is the desired material; however, estimates based on the MALDI-TOF MS data suggest a number of defects including failed conjugation at some sites is likely and that up to ~10 defect structures may contribute to approximately 50% of the sample.[81]

CHARACTERIZING POLYMER–CONJUGATE HETEROGENEITY

Heterogeneity in theranostics resulting from polymer conjugation is often overlooked, underestimated, or simply not addressed due to the difficulty in assessing it with available characterization tools. Many studies in the literature generate an equivalent to that in the cartoon in Figure 1 via experimental values that give an ensemble ligand-to-scaffold average value for the sample, such as nuclear magnetic resonance (NMR), optical absorption (UV/vis), and infrared (IR) spectroscopies or elemental analysis. Although a good starting point, ensemble averages are of limited value since they provide no information about the distribution of species present. Even for physical techniques capable of measuring the distribution of products, such as chromatography,[15,83] photobleaching,[84] and mass spectrometry,[63] characterization of conjugation distribution remains challenging in the presence of scaffold mass and structural dispersity. For example, PAMAM dendrimers, often touted as having a low polydispersity index (PDI) with values reported well less than 1.1,[85,86] still have significant branching defects. The G5 PAMAM with theoretical MW of about 29 000 Da consists of a species with a mass range of ~8000 Da, even after oligomer and trailing defects are removed.[86] This means that the distribution of molecular weights generated by multivalent attachment of typical drugs and dyes (200–500 Da) is generally a factor of 2 to 10 narrower than the mass distribution of the dendrimer scaffold itself. Mass spectrometry and size-exclusion chromatography are generally incapable of distinguishing the unique species contributing to the distribution under this set of conditions.[14,15] In addition, for mass spectrometry to be successful quantitatively, all species must have the same ionization probability. For these reasons, analytical methods that can decouple the scaffold MW distribution from the conjugation MW distribution arising from conjugation statistics are needed. Recently, we demonstrated that reverse-phase high performance liquid chromatography (rp-HPLC), in which hydrophobic ligands (i.e., small molecules such as dye, drugs, and targeting ligands or precursors with orthogonal functionality) provide a separation mechanism when conjugated to a hydrophilic scaffold (i.e., PAMAM dendrimer), can be used to quantify the conjugation distribution (Figure 5).[14,15,83,87,88] Simanek et al. have shown that rp-HPLC can be used to quantify distributions of PEG ligands on triazine dendrimers.[89] The mean, median, mode, and full distribution of ligand/dendrimer ratios present within a sample are readily ascertained. In order to obtain such data, the chromatographic methods employed (i.e., stationary phase selection, mobile phase gradient development) must be tailored

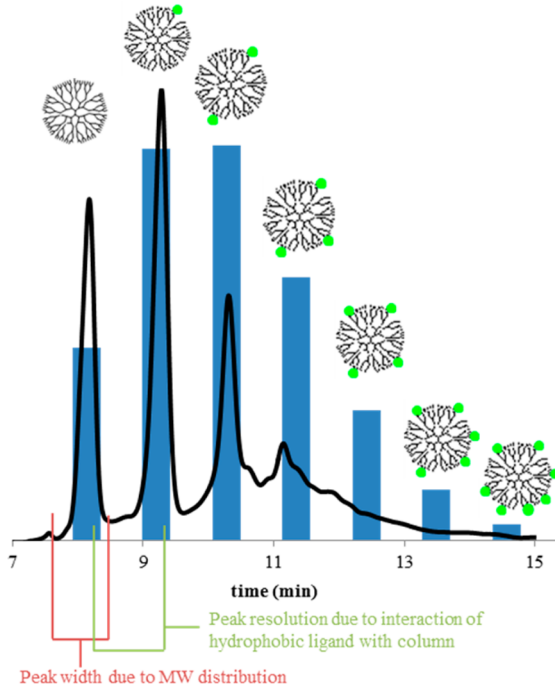

Figure 5. HPLC chromatogram of an average conjugate overlaid with the predicted distribution for an average of two ligands per particle.

to resolve the entities such that the separation obtained per hydrophobic ligand conjugated to the scaffold is greater than the peak width generated by the MW distribution (Figure 5). Experimentally optimizing such chromatographic analyses can be time-consuming. Scaffolds with large PDI result in too large a peak width for the hydrophobic ligands to overcome. In addition, some ligands of great interest (for example, folic acid) do not yield the desired separation. Hakem et al. have demonstrated that the distribution of PEG chains multivalently conjugated to a protein (trypsin) can be determined by mass spectrometry.[63] Although it is a powerful tool, the applicability of mass spectrometry is limited, like chromatography, by the ability to resolve mass differences within the scaffold (small in the case of a protein) from mass differences from ligand-to-scaffold ratios (large in the case of a 3.5 kDa or larger polymeric ligand such as PEG). Casanova et al. have demonstrated that stepwise photobleaching can be used to precisely count the number of fluorescent proteins multivalently conjugated to a single quantum dot within a distribution.[84] This technique, while showing excellent agreement with ensemble averages, is limited to fluorescing ligands and cannot be applied to many drug or targeting entities of interest. Despite some limitations, these approaches offer a powerful window into the details of conjugate heterogeneity for some classes of bioconjugates.

The discussion so far has assumed perfectly random conjugation statistics. A number of factors, including mass transport, solubility, autocatalysis, cooperativity in binding, and steric blocking of sites, may cause deviation from Poisson statistics.[14,63,87] Such perturbations can lead to significant differences in ligand-to-scaffold ratio distributions and yet go undetected by measurements of ensemble averages. Mullen et al. experimentally examined how mass transport could affect the observed distribution of ligand/polymer ratios.[14,62] Figure 6 gives examples of excellent ligand-to-scaffold mixing, yielding distributions similar to theoretically expected Poisson distribution (PD) ratios, and poor ligand-to-scaffold mixing, resulting

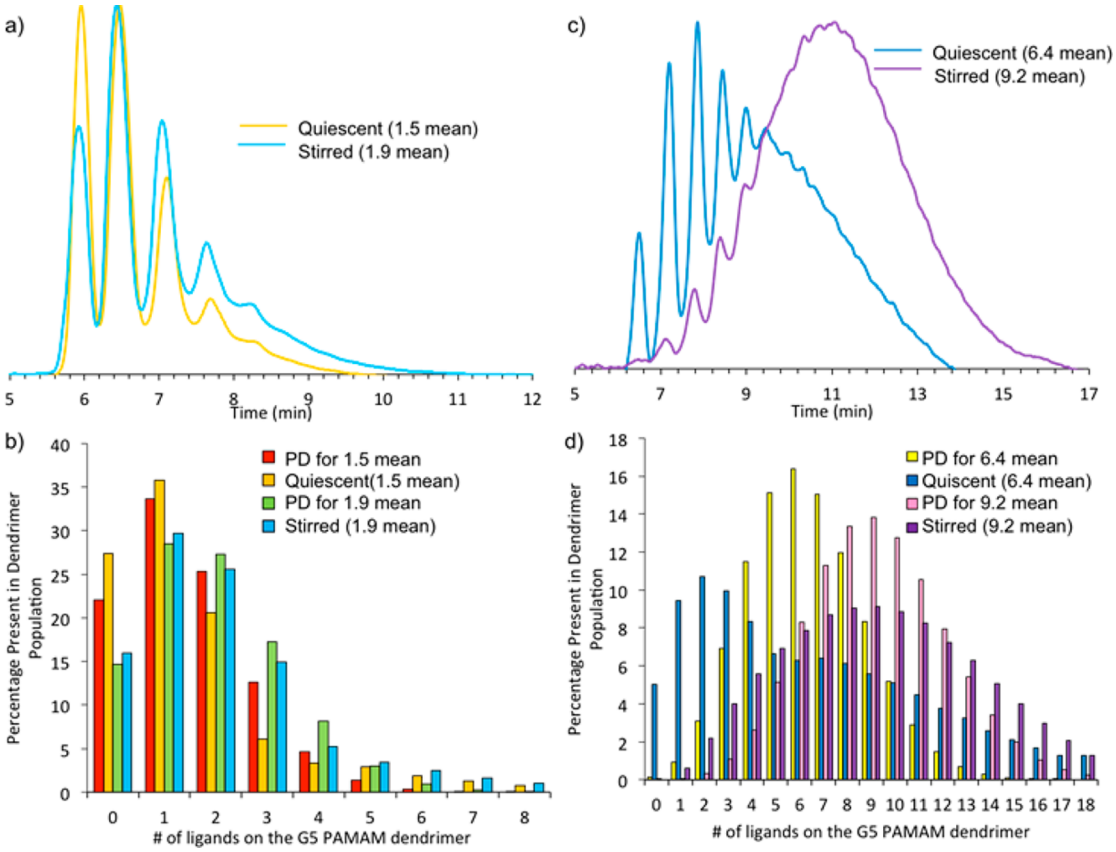

Figure 6. Variation in ligand-to-scaffold distribution as a function of ligand-to-scaffold ratio and mass transport. The model system employed was the conjugation of 3-(4-(2-azidoethoxy)phenyl)propanoic acid to G5 PAMAM dendrimer. (a) rp-UPLC trace of 2.5 equiv/dendrimer yielding mean ligand-to-scaffold ratios of 1.5 (yellow) and 1.9 (cyan). (b) Distribution obtained from fitting UPLC trace in panel a and Poisson Distribution (PD) based on mean ligand-to-scaffold ratio. (c) rp-UPLC trace of 9 equiv/dendrimer yielding mean ligand-to-scaffold ratios of 6.4 (blue) and 9.2 (purple). (d) Distribution obtained from fitting UPLC trace in panel c and PD based on mean ligand-to-scaffold ratio. See ref 62 for synthetic details and refs 14 and 87 for chromatography details.

in concentration gradients within the reactor. For both examples, the largest impact on the ligand-to-scaffold distribution for a given mean value is the effectiveness of mass transport during the reaction. As is illustrated in Figure 6, poor mass transport results in a wider distribution of ligand-to-scaffold ratios, with this effect getting more pronounced as the mean ligand-to-scaffold ratio increases. Even in the well-stirred case, the percentage of high ligand-to-scaffold ratios exceeds the theoretical value because this popular conjugation chemistry is autocatalyzed by the conjugation product.[88]

IMPACT OF CONJUGATION HETEROGENEITY ON MULTIVALENT BEHAVIOR

The modes of multivalent binding have been thoroughly reviewed elsewhere.[90,91] Briefly, three mechanisms are generally described to explain the favorable influence of multivalency on binding kinetics (Figure 7). The first mechanism is effective concentration. Attaching multiple copies of a ligand to a single scaffold, particularly a dendritic architecture, can "prepay" the entropic penalty of achieving high local concentrations. This local increase in concentration is higher than the equivalent solution concentration containing the same amount of free ligand, as the scaffold immobilizes the ligand in a defined volume (Figure 7a). Statistical rebinding describes the increased chance of a reattachment of the ligand/target interaction upon dissociation of the initial event, due to the high local ligand concentration (Figure 7b). The localization of additional ligands increases the chances that, upon dissociation of the initial reaction, the same polymer-conjugate will rebind to the protein. Both of these concentration-dependent mechanisms become important when considering sample populations like those in Figure 6. In particular, for the reaction carried out by mixing 9 equiv of ligand-to-scaffold, the sample with poor mass transport (Figure 6c) has significantly more unfunctionalized, monofunctional, and bifunctional material, which will have distinctly different binding behavior as the effective concentration is much lower and rebinding events are less favored. The third mechanism, the chelate effect, describes the ability of a multivalent conjugate to undergo multiple binding interactions, which can increase avidity more than the sum of the independent interactions (Figure 7c). This mechanism, which is likely the first that comes to mind when discussing multivalency, can be achieved by >99% of the population for the well-mixed sample (purple) but only 86% of the poorly mixed sample (blue) (Figure 6c). These mechanisms work together, and large differences in behavior as a function of sample distributions can be expected.

MEASURING MULTIVALENT BEHAVIOR

Multivalent conjugates are often touted as having favorable kinetic, thermodynamic, and biological activity compared to that of their monovalent and/or small molecule counterparts.[92−94] This behavior is typically demonstrated by *ex vivo* and *in vitro* methodologies that show an increase in a desired

dx.doi.org/10.1021/bm500921q | *Biomacromolecules* 2014, 15, 3215−3234

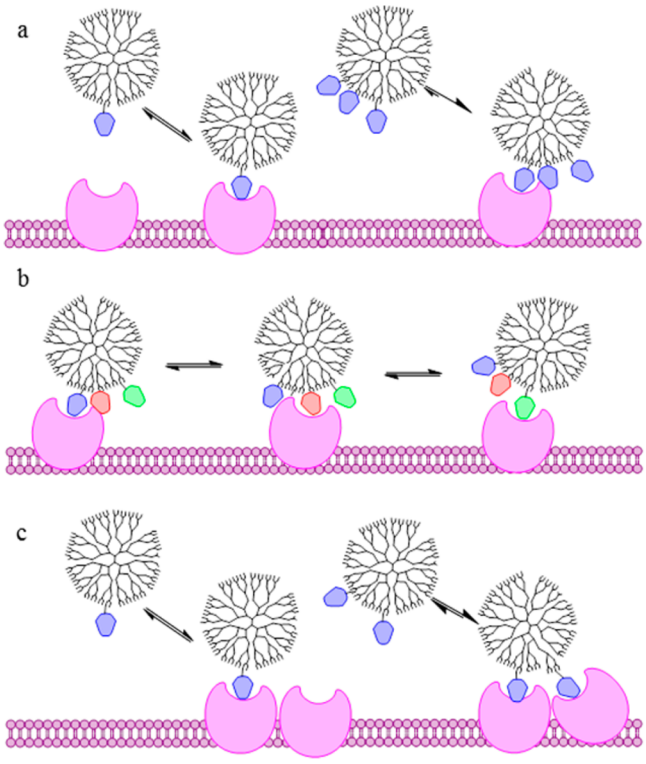

Figure 7. Multivalent binding mechanisms (a) Effective concentration increases chances of binding. (b) Statistical rebinding is higher for multivalent conjugates if the original interaction dissociates. (c) The chelate effect allows for multiple interactions through one conjugate.

behavior (i.e., binding, inhibition, toxicity) for the conjugate species. Problematically, like many characterization techniques, methods used to evaluate these desired functions are typically incapable of measuring the contributions from the species within a sample distribution and instead assess the overall ensemble impact. Surface plasmon resonance (SPR) binding measurements are employed to measure the association and dissociation rates of multivalent ligand-conjugates being flowed over a surface functionalized with receptor.[95−98] Although binding or dissociation of a unique conjugate is measured by this sensitive technique, the signal observed is the summation of all simultaneous events. Thermodynamic information about multivalent interactions can be measured by isothermal titration calorimetry (ITC), which measures the enthalpy and stoichiometry of binding in solution;[99] however, the values obtained are averaged across all species in solution. For example, assays of biological activity to measure cellular uptake,[100−102] activity inhibition,[103−106] or cytotoxicity[31] of a conjugate, are commonly employed to demonstrate clinical advantages of multivalent conjugates. These assays can be complicated by large differences in particle hydrophobicity caused by different total numbers of ligands per particle that can substantially change biolocalization properties. In all three cases, the methods provide ensemble-level data, and it is difficult or impossible to determine the activity of individual components of the distribution.

CHALLENGES IN DEVELOPMENT AND INTERPRETATION OF MULTIVALENCY MODELS

The presence of a range of ligand-to-scaffold ratios complicates evaluation of physical models of multivalent activity. Without an understanding of the distribution of conjugates present within a sample, it becomes impossible to assign the active components in the mixture. What minimum valency is needed to accomplish a multivalent interaction on a surface? Is there a kinetic advantage to achieving higher valencies? At what valency do thermodynamic effects (i.e., reduced solubility, steric crowding) negatively impact binding? How can activity differences be explained for samples that appear the same by ensemble techniques such as NMR? Mechanistic understanding of multivalent behavior allows for the design of new conjugates with optimized behavior but, to date, has remained a significant challenge for the field.[14]

In order to highlight these challenges, let us consider a specific example from the literature. In 2007, Banaszak Holl and co-workers examined the binding of a series of stochastic G5 PAMAM conjugates of folic acid to folate binding protein via SPR.[96] A decrease in dissociation constant was observed as the average valency of the conjugate was increased from 2.6 to 13.7. The authors proposed a mechanism to explain this trend in which dissociation slows with each additional conjugated folic acid because a new ligand−protein interaction is formed (Figure 8a). However, upon further consideration of the

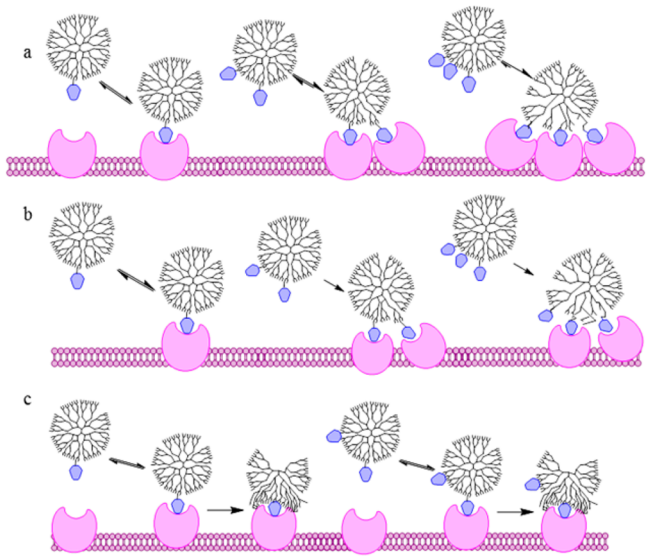

Figure 8. Three mechanisms proposed to explain G5-FA binding behavior: (a) avidity increases with valency, (b) two populations experience two different binding mechanisms, and (c) folic acid keys a stronger, nonspecific interaction between the conjugate and protein.

distributions of folic acid-to-dendrimer ratios present in such samples, the authors proposed a different mechanism.[107] This model establishes two binding populations for each sample: monovalent conjugates that are only capable of weak, reversible interactions, and multivalent conjugates with two or more folic acids that all experience a strong, irreversible binding (Figure 8b). This model attributes differences in dissociation between samples not to separate mechanisms but to the decrease in zerovalent and monovalent material as the overall average increases (Figure 9). A third model was proposed by Licata and Tkachenko in 2008.[108] This model attributes the increased interaction of the conjugate to be due to van der Waals interactions between the protein and dendritic scaffold. The polymer−protein interactions must initially be keyed by a single, specific interaction of folic acid and folate binding

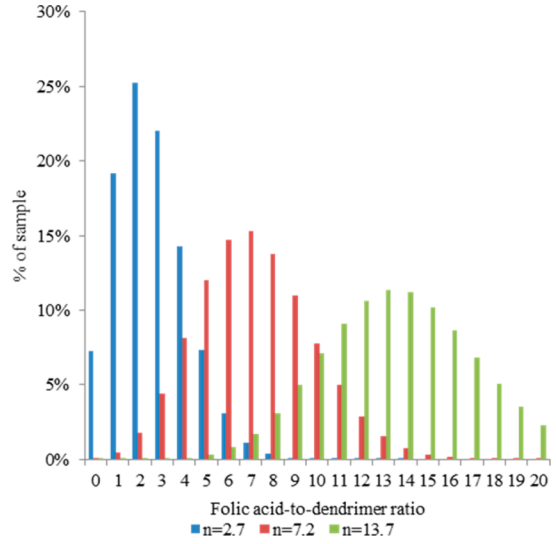

Figure 9. Poisson distributions for the three G5-FA conjugates discussed by Hong et al.,[96] Waddell et al.,[107] and Licata et al.[108]

protein but do not depend on multivalent folic acid interactions with the SPR surface (Figure 8c).

Recently, van Dongen, Banaszak Holl et al. had success in isolating samples of G5-FA_n conjugates containing non-stochastic distributions including a sample that was >95% G5-FA_1.[109] Using these materials, experiments confirmed the proposed mechanism of Licata and Tkachenko as being the most consistent and ruled out both hypotheses based on multivalent FA interactions. For *in vitro* interactions with folate binding protein, multivalent display of FA ligands did not increase the binding constant appreciably and had only minor effects via increasing overall concentration of FA in solution. Indeed, it was confirmed that the previously hypothesized "strong multivalent binding"[96] could be obtained with only a single FA per polymer scaffold as illustrated in Figure 8c. In this case, elimination of the Poisson distribution was crucial for obtaining clear experimental results.

This example shows that the presence of a single ligand-to-scaffold distribution can be challenging. Earlier, problems due to multiple conjugations were introduced, such as the presence of nontargeted particles, invisible particles without dye, or monovalent drugs without improved activity profiles. The possible effects of both single and multiple ligand-to-scaffold distributions will be further examined in the next section.

IMPACTS OF CONJUGATE HETEROGENEITY IN BIOLOGICAL APPLICATIONS

Targeting, Specificity, and Biodistribution. In 2011, a simulation study by Martinez-Veracoechea and Frenkel discussed how ligand valency, binding strength, and level of receptor expression affect specificity of binding.[110] The authors concluded that monovalent conjugates had no specificity regardless of receptor density and that adsorption varies linearly with receptor density. Multivalent conjugates, by contrast, exhibit superselective behavior (i.e., adsorption increases much faster than linearly with receptor density). Therefore, low concentrations of multivalent conjugates can specifically target cell surfaces that are overexpressing a receptor protein, without affecting low-expressing, healthy cells. However, stochastic multivalent conjugates with average ligand-to-scaffold ratios of ∼5 or less have significant populations of unfunctionalized or monovalent conjugates. The monovalent species will bind to healthy or unhealthy cells equally and may still be uptaken via a receptor-mediated pathway. More generally, the presence of a Poisson distribution of ligand per scaffold will make it more difficult to match a number of nanoparticle-conjugated ligands to available cell receptors, therefore achieving optimal superselectivity.

The degree of valency of hydrophobic ligands influences the localization of a conjugate within a patient's body, tissue, or cells because surface hydrophobicity is a key factor for both opsonization and immune response as well as endocytosis pathways upon cell entry.[111−113] In general, more hydrophobicity is believed to correlate with a greater degree of protein coating and a more rapid clearing by the reticuloendothelial system (RES). The potential activation of multiple biological pathways and system-wide responses *in vivo* creates a substantial challenge to the understanding of stochastic mixtures containing a distribution of surface hydrophobicity.

Therapeutic Effects. Beyond localization effects, the therapeutic effect of conjugates has been shown to vary as an effect of valency. The simplest mode of therapeutic enhancement is the delivery of a higher drug payload to a single cell than the monovalent equivalent. The amount of drug delivered, of course, varies directly with conjugate valency and therefore a conjugate with a distribution of drug-to-scaffold ratios will exhibit a distribution of effective enhancement, with the measured enhancement being the average valency. For example, higher cytotoxicities are reported for PAMAM−methotrexate conjugates when the valency is increased from 5 to 10.[79] However, a study by DeSimone et al.[114] observed a new behavior at high valency that was not observed at all in low-valency conjugates or the monovalent ligand by itself. The authors demonstrated that nontoxic transferrin and transferrin antibodies, which are employed as ligands to target various cancers for drug delivery, exhibit selective toxicity to a Ramos lymphoma cell when multivalently conjugated to a PRINT nanoparticle, while remaining nontoxic to solid tumor cells and healthy kidney cells. In this case, a mean of 1200 transferrin proteins are conjugated to an estimated 1 200 000 surface sites (0.1% coverage), giving a Poisson distribution of transferrin per particle assuming good mixing in the conjugation reactions. The exhibition of novel behaviors at high valencies can create subpopulations within a sample with entirely unique properties.

Imaging Agents. Organic dyes are used as fluorescent probes in order to image biological processes; however, organic dyes are prone to photobleaching and self-quenching. In order to improve aqueous solubility, provide targeting properties, or provide a label, dyes are frequently conjugated to polymer scaffolds.[115] When these conjugations are performed under stochastic reaction conditions, Poisson distributions of dye/scaffold ratio result, as highlighted in Figures 3−6 and 9. Dye−dye interactions have long been understood to impact photophysical properties, and these effects are readily measured.[116] Therefore, substantial efforts have gone into controlling and understanding dye/scaffold ratios. Mier et al. studied the stochastic conjugation of multiple dyes to PAMAM dendrimer including fluorescein, rhodamine, coumarin, and dansyl.[66] With the exception of dansyl, they found that fluorescence intensity decreased with an increasing mean number of dyes due to a combination of a small Stokes shift and the high effective concentration that results from multiple dyes conjugated to the same polymer core. By way of contrast, in dansyl-modified PAMAM materials, fluorescence increased

dx.doi.org/10.1021/bm500921q | *Biomacromolecules* 2014, 15, 3215−3234

along with increasing dye/dendrimer ratio, presumably due to the large Stokes shift of 195 nm. Schroeder et al. examined Cy3 and Cy5 dye optical properties conjugated to G5 PAMAM or G6 PAMAM dendrimer in order to create a new set of materials for biological imaging with enhanced stability and increased accuracy in single-molecule imaging.[117] Dendrimer mixtures with an average of 8 Cy5 dyes gave slower photobleaching compared to that of free dye, with a 6−10-fold increase in the photobleaching lifetime value for G5 PAMAM. The dendrimers with an average of 14 Cy5 dyes on G6 PAMAM showed a ∼17-fold increase in photobleaching lifetime value. Note that the average conjugation numbers used in this case will generate mixtures with <0.5% of the material having zero or one dye, thus helping to eliminate the most dramatic difference in effective local concentration, and thus photophysical properties, that typically occur as a dye/polymer ratio is varied. Wagner et al. employed stochastically prepared G3 PAMAM dendrimer conjugated to a mean of 1 Alexa Fluor 555 dye to quantify the rate constant of dendrimer uptake in Caplan-1 cells.[118] Assuming a Poisson distribution, this material should have about 37% of the dendrimer containing no dye, 37%, one dye, 18%, two dyes, and 6%, three dyes. Interestingly, rp-HPLC did not resolve different species as being present in this case, although separation is possible for other dye ligands.[14,65] In this study, both the average uptake rate for the dye conjugate materials and the predicted efflux rate were reported on the basis of measurements of the mean fluorescence of the mixture. Differences in dye fluorescence as a function of conjugation number per dendrimer particle[65,66,117] were not addressed as part of the study. For all of these imaging studies, the presence of the large number of hydrophobic dye molecules per dendrimer may itself substantially impact the biological behavior of all of these samples.[111,112] Understanding the role of biodistribution for such species represents a major challenge for the application of these materials.

APPROACHES TO OVERCOMING HETEROGENEITY PROBLEMS IN MULTIVALENT CONJUGATES

As indicated above, mixtures of ligand-to-scaffold ratios can complicate the synthesis, evaluation, and clinical application of multivalent conjugates. A number of synthetic strategies to overcome this problem have been employed (Figure 10). Methods employed include using high densities of functional ligands to avoid under-modified populations with limited activity,[66,104,106,117,119−121] techniques that create clusters of ligands to optimize local concentration effects,[122−124] and the synthesis of precise conjugates, using biologically inspired scaffolds[125−127] and both bottom-up[59,98] and top-down (or convergent[128,129] and divergent,[65] in the case of dendrimers) synthetic approaches, in which all species in the sample have the same ligand-to-scaffold ratio. In this section, we will provide a brief review of some successful applications of controlled multivalent conjugates over the last 10 years.

High Density Conjugates. At high percentages of modification, and assuming ideal or close to ideal conjugations (to avoid nonideal populations like the example in Figure 6), the amount of unmodified and low-average conjugates becomes minimal, allowing for benefits of effective concentration based multivalent behavior. The average distances between conjugated ligands on a scaffold also decreases, and at some point it can be assumed that the ability to have chelate effect type multivalent interaction is limited by the scaffold size and not the relative location of the ligands.

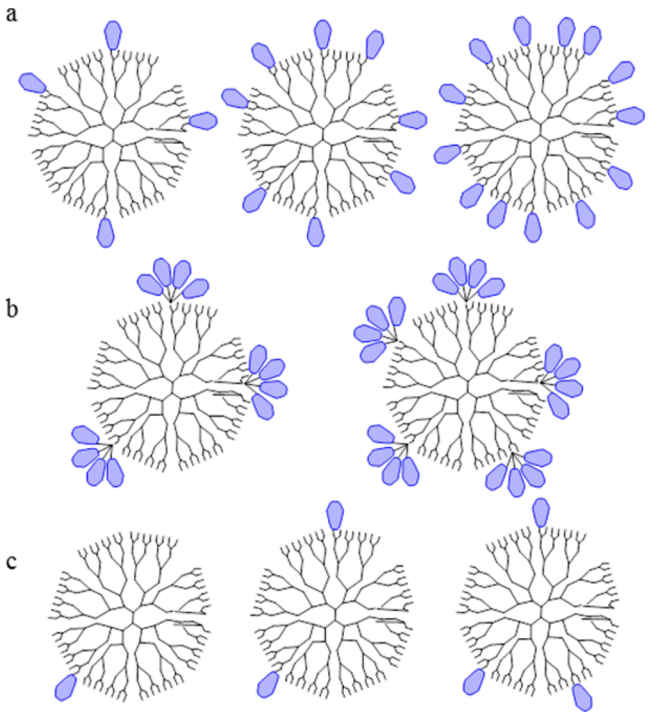

Figure 10. Synthetic approaches to controlling multivalency resulting from ligand conjugation to polymer scaffolds include (a) ligand density variation, (b) ligand clustering, and (c) those that result in precise ligand-to-scaffold ratio structures.

Exhaustive Conversion of Small Numbers of Terminal Reaction Sites. A number of strategies have been implemented to reduce or eliminate distributions of ligand-to-scaffold ratios. In the resulting conjugates, heterogeneity is limited by the scaffold polydispersity instead of conjugate distributions. For example, polymers containing a small number of arms containing reactive sites can be exhaustively reacted to give integer multiples of the number of terminal groups.[121] This strategy was introduced earlier in the discussion of the G4 PLL dendrimer with napththalene disulfonic acid conjugated to the surface (SPL7013) developed by Starpharma as VivaGel.[80−82] A similar approach was employed to exhaustively funtionalize G4 PLL with PEG[130] and with a 1:1 ratio of PEG and MTX using a preformed linker containing each ligand.[131,132] A recent report from Szoka et al. illustrates this strategy in a system that allows facile variation of scaffold molecular weight, appears to be scalable, and could be readily extended to explore various ligand-to-scaffold ratios (Figure 11).[133] Atom transfer radical polymerization (ATRP) was employed to grow eight poly(ethylene glycol) methyl methacrylate (PEGMA) arms from a

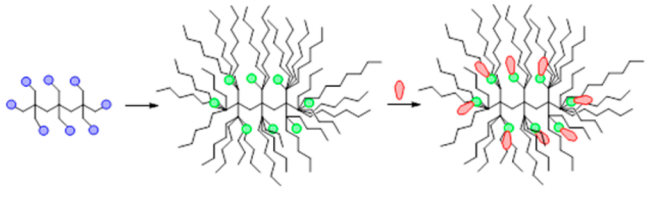

Figure 11. Use of tripentaerythritol core to control number of functional arms for a star topology polymer.

dx.doi.org/10.1021/bm500921q | Biomacromolecules 2014, 15, 3215−3234

tripentaerythritol core. Subsequent stoichiometric conjugation of doxorubicin to the ~45 kDa core yielded an average 5−8 doxorubicin per star-comb polymer, as determined by optical absorption measurements. Another notable example of exhaustive conversion of reaction sites with functional ligands is glycopolymers.[134−138] This class of polymers exhibits the cluster glycoside effect, which is broadly used to describe the enhanced binding and activity of multivalent carbohydrates compared to the monovalent equivalent to proteins involved in a variety of biological events.[139] Although linear and graft glycopolymers with low polydiserpsities have been successfully synthesized,[140,141] these samples still represent a significant range of valencies due to the nature of the polymer scaffolds. Attempts to prepare monodisperse glycopolymers have been made via taking advantage of the dendrimer architecture, which can, theoretically, be synthesized as molecularly pure. The surface groups of the dendrimer are 100% modified with a saccharide via coupling or click chemistry, using an excess of the saccharide to ensure full conversion. In this way, absolute valency can be controlled by generation number, as the number of end groups scales with generation.[60] For example, in recent work by Jayaraman et al.,[119] generation 2, 3, 4, and 5 glycodendrimers were prepared with an expected 4, 8, 16, and 32 mannos-6-phosphate valency, respectively. These structures were confirmed by NMR spectroscopy; however, mass spectrometry and elemental analysis failed due to the large nature of the structures. The larger dendrimers had less-than-expected valencies (15 and 28, respectively). This example demonstrates the limit of such approaches in obtaining homogeneous structures. As indicated by previous reports,[85,86,142] inter- and intramolecular loop formations during dendrimer synthesis can create a distribution of defect species within a dendrimer. The resulting valencies after 100% modification with functional groups such as saccharides are still a distribution, reflecting the distribution of defect species in the dendrimer scaffold. Without further structural characterization of the scaffold, it is difficult to determine if the coupling reactions of Jayaraman et al. failed to go to completion, leaving unreacted carboxylic acids on the dendrimer, due to steric crowding. It is more likely, however, that this observation is actually a reflection of heterogeneity in the scaffold (PAMAM dendrimer), which is known to contain skeletal defects which reduce the average number of reactive groups by more than 25% by generation 5.[86,143] Another recent example of glycodendrimers by Riguera et al.[104] highlights the inherent coupling of conjugate size and valency by this technique. Generation 1−3 dendrimers with 3, 9, or 27 surface conjugated mannose units were prepared and evaluated by SPR for the ability to bind to high- and low-density Concanavalin A (ConA) surfaces. In this work, two separate binding mechanisms were observed: low-affinity binding for all generations on the low-density protein surface and high-affinity binding for only the largest dendrimer on the high-density surface. The authors point out that the distance between proteins on the low-density surface is greater than the diameter of any of the dendrimers and that the only multivalent effects possible are based on effective concentration and rebinding. However, the distance between the proteins on the high-density surface allows for only the generation 3 structure to experience the chelate effect, breaching the distance between two proteins on the surface. However, this work cannot determine what, if any, multivalent effects a larger, but lower valency, dendrimer would experience, and whether there is any additional benefit to fully functionalizing the dendrimer surface or if there is a threshold valency for chelate interactions.

Other scaffolds have been exhaustively converted to achieve the glycoside cluster effect. Renaudet et al.[106] employed a dendrimer-like multivalent display of mannose. Their findings confirmed that display of 16 carbohydrates showed more multivalent interactions than that of a corresponding tetravalent unit (Figure 12). However, this work also used two linking

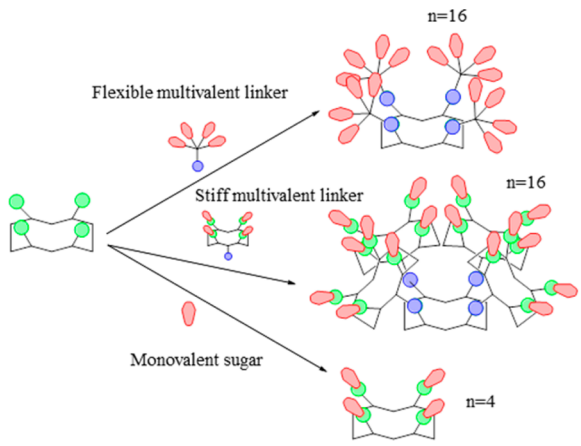

Figure 12. Dendri-RAFTs of mannose valencies 4 or 16. Higher valencies were tested with both stiff and flexible linkers.

systems to combine the four tetraclusters and showed a significant enhancement of multivalent interaction with ConA with a more flexible linker. This observation hints at the importance of scaffold architecture in multivalent binding, a topic that will not be further explored here.

Other ligands beyond glycosides have been used to exhaustively convert multivalent scaffolds. Mier et al. exhaustively converted PAMAM dendrimers to saturated numbers of dansyl dyes.[66] Fei et al. exhaustively treated G2 PAMAM dendrons with thiazole orange.[144] Dendrons were also used as scaffolds for multivalent peptides by Welsh and Smith.[120] First- and second-generation dendrons fully converted to precisely 3 and 9 Arg-Gly-Asp peptides were prepared and evaluated for integrin binding affinity as a potential cancer targeting agent. Although the trivalent dendron showed enhanced affinity compared to that of the equivalent monovalent peptide, the higher valency generation 2 dendron had lower affinity for the integrin. The authors speculate that this trend is due to steric crowding of the ligands, interfering with the interaction between the peptide and target. This study emphasizes the importance of identifying the ideal valency for complex biological systems, as apparently more is not always better.

As indicated by the peptide−dendron example, the higher-valency-is-better approach is not always optimal for multivalent activity. Complete conversion of the scaffold is not always ideal, either. Not all ligands can be solvated at such high valencies, and nontoxic ligands may become toxic at high valencies, as discussed earlier,[114] which may not be a desirable trait. Therefore, the distribution of species problem created by less-than-full conversions has been addressed by Choi and co-workers by systematically increasing the ligand density to reach desired activity levels while maintaining conjugate properties such as solubility.[79] This approach allows for the comparison of the multivalent behavior at low-average and high-average

dx.doi.org/10.1021/bm500921q | *Biomacromolecules* 2014, 15, 3215−3234

valencies. In addition to the PAMAM−folic acid example detailed in an earlier section[100] and the related G5 PAMAM conjugates to methotrexate (Figure 13a),[79] Choi and co-workers reported a SPR study of a vancomycin conjugates. Several ligand-to-scaffold ratios ranging from 1.2 to 8.3 (Figure 13b) were tested for the ability to bind to surfaces that mimicked vancomycin susceptible and resistant bacteria.[32] Although free vancomycin did not significantly bind to the "resistant" surface, all of the multivalent conjugates did. Interestingly, the strength of binding was not influenced by valency, even when the average valency was increased from 1.2 to 8.3, a reduction of the monovalent population from around 180 particles of 500 (36%) to less than 1 in 500 (0.2%). This observation suggests that either the monovalent species is not participating at all in the binding and therefore is not observed or that the mechanism of binding depends on the attachment of a single ligand to the scaffold, inducing a further scaffold/surface interaction, and not on the valency (similar to the proposed mechanism for PAMAM−folic acid in Figure 8c). A purely monovalent conjugate without the presence of a distribution would be necessary to distinguish between these mechanisms. As demonstrated by these examples, employing high-ligand-density samples is an approach that can be successful in creating conjugates with the desired properties, but it does not generally lead to clear mechanistic insights of the systems being studied.

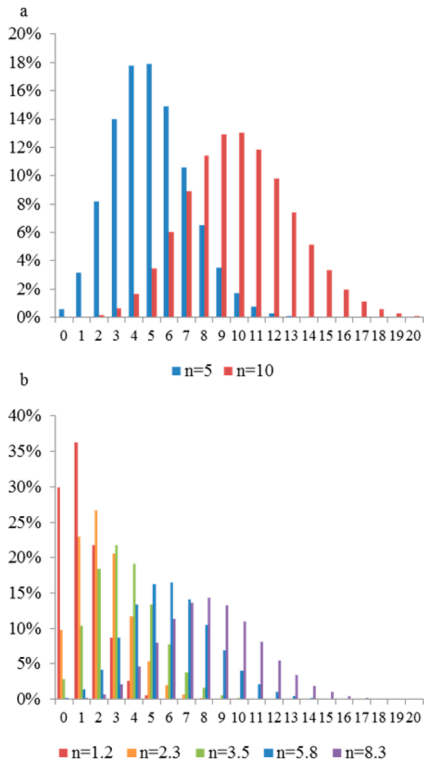

Figure 13. Distributions present in multivalent conjugates of PAMAM to (a) 5 or 10 methotrexates and (b) various amounts of vancomycin.

Ligand Clustering. High ligand densities are in part successful because they maximize local concentration and statistical rebinding mechanisms of multivalency. However, exhaustive conversion of reaction sites is not possible for many ligand-to-scaffold systems due to challenges with solubility and steric crowding and biological effects related to opsonization and biodistribution.[111,112] An approach to increase local ligand concentrations without fully functionalizing a surface is to create patches or clusters of the ligand on the scaffold (Figure 10b). In a recent study by Gillies et al.,[122] polymer vesicles were functionalized with dendritic clusters of ∼7 mannose units (Figure 14b). The surface density of clusters was also varied by controlling the amount of azido-functionalized polymer in the vesicle scaffold to give statistical distributions. As a control, the same vesicles were functionalized with a nonclustered, monomeric azido-modified mannose to create multivalent mannose structures that did not have the localization effects of the dendritic clusters (Figure 14a). The vesicles were evaluated by a hemagglutination assay, which measured the ability of the vesicles to inhibit red blood cell clustering by selectively binding the ConA. When compared to free mannose, the multivalent but nonclustered vesicle had approximately 4 times the activity as free mannose relative to the amount of mannose present, likely due to a chelate-type interaction. However, the activity of the equivalent cluster functionalized vesicle was over 40 times that of the monomer on a mannose-to-mannose basis. This example highlights the importance of controlling the spatial distribution of ligands on a scaffold system for such systems. In another example, Pine and co-workers recently published methods to synthesize polymeric scaffolds with localized, directional binding patches.[123] In this work, colloidal particles were prepared from nanoclusters with 1−7 amidine patches in symmetric orientations. The original work utilized these selectively active sites to assemble larger nanostructures; however, the translation of these sites to directional multivalent binding scaffolds is clear. Complete functionalization of these sites with multivalent ligands would create areas of high local concentration, and multiple patch sites allow for well-defined, chelate-type cross-linking. Other scaffolds, such as PAMAM dendrimers, are more flexible than the cross-linked vesicle, which allows the ligands to be localized even if they are bound on different polymer branches.[145]

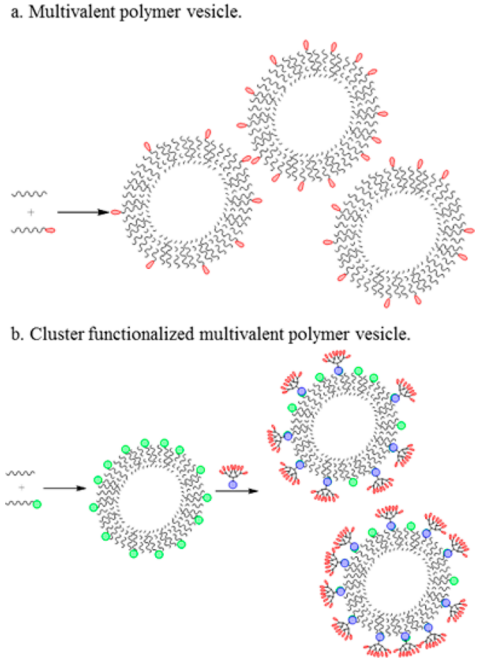

Figure 14. Mannose-functionalized vesicles prepared as (a) single mannose units and (b) clustered mannose units.

dx.doi.org/10.1021/bm500921q | *Biomacromolecules* 2014, 15, 3215−3234

However, creating bifunctional conjugates (e.g., with a drug and a targeting ligand) still creates a more heterogeneous population. In 2012, Baker et al.[124] synthesized triazine-based clusters of a single folic acid (targeting ligand) and a single methotrexate (drug ligand) with an azide click chemistry group. These clusters were then clicked to a previously synthesized, stochastic distribution of dendrimer-alkyne click ligand conjugate. In the resulting product, which still contained a distribution of ligand-to-scaffold ratios, each unique species contained the same proportion of drugs and target ligands. There is a reduction in unique species from ∼170 in the equivalent, double-conjugation approach (Figure 15a) to ∼13

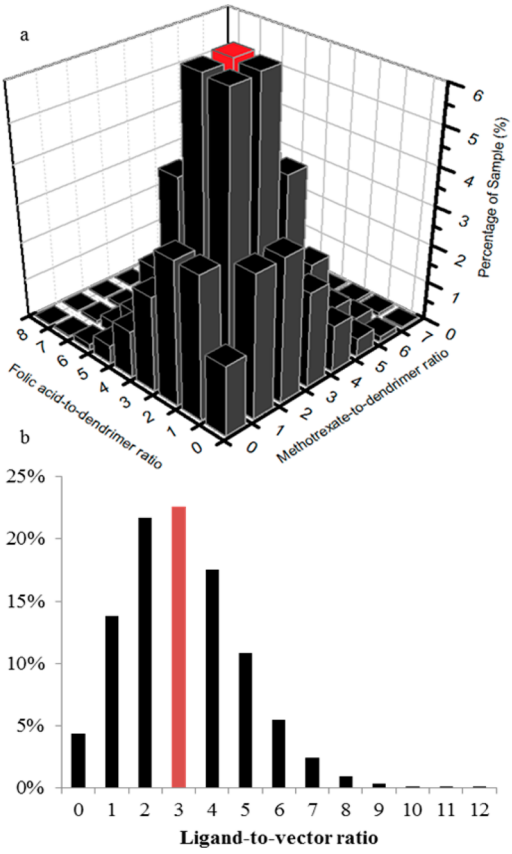

Figure 15. Product species present in (a) a double conjugation of methotrexate and folic acid and (b) the single conjugation of the bivalent cluster. In each case, the mean number of ligands is highlighted in red.

by employing only one conjugation (Figure 15b). Importantly, the single distribution conjugate exhibited higher growth inhibition for KB cells than a double-conjugation sample, the latter of which actually had a slightly higher methotrexate valency. This result is possibly due to the elimination of untargeted treatment populations and drugless but targeted species from the sample. In this case, presence of a larger distribution of samples actually counteracts the benefits of multivalency. This example emphasizes the importance of considering the activity impacts of complicated, sequential synthesis of multifunctional systems.

Precise Ligand-to-Scaffold Ratio Conjugates. Although high-density surfaces and ligand clustering improve conjugate behavior, mechanistic assignment of activity and identification of populations with optimal behavior are best done with homogeneous samples. The presence of a heterogeneous mixture of products in these approaches (except for full conversion of perfectly homogeneous scaffolds) may also present complications in scale-up, prevent clinical application, or fail to meet FDA requirements for approval. Therefore, several strategies, which can be broadly categorized as biologically inspired approaches, bottom-up (or convergent dendrimer) approaches, and top-down (divergent dendrimer) approaches, have been employed to synthesize multivalent conjugates in which all species present have the same ligand-to-scaffold ratio.

One approach is to add detergent to solubilize well-defined, hydrophobic dendrimers, as was demonstrated for the case of polyphenylene dendrimers containing well-defined numbers of dye molecules.[146] Another approach is to make the hydrophobic group the core of the polymer scaffold. This goal has been achieved using a perylenediimide core and polyester dendritic arms by Yin et al.[147] and using fluorescein or perylenediimide cores and polyglycerol arms by Zimmerman et al.[148] Placing the dye at the core resolves concerns about hydrophobic variation at the dendrimer surface; however, it restricts the polymer particle to a single fluorophore. Florence et al. also demonstrated that this goal could be achieved by synthesizing a branched lysine dendrimer that was intrinsically fluorescent.[149]

Several groups have taken advantage of the homogeneity of biological nanoparticles as precise scaffolds and protein oligomers as well-defined arms. Proteins are of great interest as multivalent scaffolds because their nanoscale size allows them to span large areas for chelate effect binding, the well-defined structure allows for precise functionalization, and the protein itself has therapeutic potential. One such application by Zhang and co-workers employed a tetrameric far-red fluorescent protein (tfRFP) as both an imaging agent and a scaffold conjugated multivalently to cancer targeting peptides (Figure 16a).[125] The N and C termini of each unit in the tfRFP were conjugated to 14-mer targeting peptides to create conjugates consisting of exactly 8 targeting peptides per tfRFP. By way of comparison, random conjugation of an average of one fluorescent probe and 8 peptides to an excess of polymer attachment sites would result in over 300 unique combinations, of which over 30% would not contain an imaging agent. Conjugation of the peptides to the tfRFP significantly increased the uptake of the probe, although it was shown to decrease the fluorescent intensity of the tfFRP. The location and number of functionalizable sites limits the placement of multivalent ligands on proteins, however, which may not allow for optimal effective concentration enhancements. Ikkala et al. addressed this challenge by utilizing dendrons of varying generations to create DNA binding patches of varying valency on two different protein scaffolds, bovine serum albumin (BSA), and a genetically engineered Class II hydrophobin (HFBI) (Figure 16b).[126] This work takes advantage of a single cysteine residue available on each protein for thiol reactions to the dendrons. Employing dendrons with 3 or 9 surface primary amines allows for precise valency control of the resulting conjugate. Although there was only a 50% yield for the BSA scaffold (due to oxidation of the cysteine), the purified products contained a single dendron per protein. The DNA binding of the conjugates were then evaluated by an ethidium bromide displacement assay. The unmodified proteins did not bind the DNA, whereas the conjugates bound the DNA to varying degrees. The smaller HFBI conjugates had relatively higher

dx.doi.org/10.1021/bm500921q | *Biomacromolecules* 2014, 15, 3215−3234

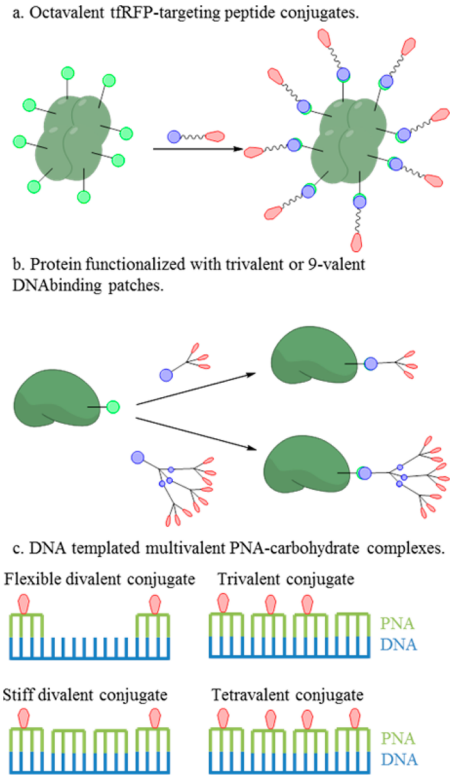

Figure 16. Conjugation valence controlled using a biological scaffold: (a) octavalent protein core, (b) monovalent protein core with differing dendron valency, and (c) DNA templating for control of polymer valence and ligand spacing.

affinity compared to that of the larger BSA conjugates, which the authors attributed to the differences in dendron-to-protein size (which could translate to a percent functionalization effect). As expected, the higher valency of the larger dendron also promoted DNA binding.

The precise interactions of nucleic and amino acids have also been utilized to craft homogeneous multivalent structures. Seitz and co-workers recently performed a thorough proof-of-concept study proving the usefulness of DNA as a template for creating precise multivalent architectures in a bottom-up approach (Figure 16c).[150] In this work, base pairing between DNA and synthetic peptide nucleic acids modified with *N*-acetyllactosamine (LacNAc) was employed to tailor scaffolds with precisely defined valency, precisely defined spacing, and varied flexibility. The binding of LacNAc to *Ricinus communis* agglutinin (RCA_{120}) is known, with two binding sites that are ∼130 Å apart across the concave surface of the protein. As such, valency effects were studies by synthesizing complexes with 1−4 LacNAc. The strongest absolute binding, as measured by K_D, was observed for the tetravalent construct, although this sample did not have the highest relative potency per LacNAc, indicating that this enhancement was due to increased effective concentration/statistical rebinding. Two different spacers were used to vary the length between LacNAc units in divalent complexes. As expected, the spacer that more closely matched the separation of the active sites showed approximately twice the binding activity as that of the complex where the distance between the LacNAc units was too close. Finally, flexibility was evaluated be synthesizing divalent structures that were completely double stranded and partially single stranded between the LacNAc units. The less flexible complex had slightly higher binding, which may indicate unfavorable thermodynamic penalties to obtain binding conformation in the flexible complex. Biologically inspired approaches provide excellent control of scaffold heterogeneity, ligand valency, and spatial arrangement. However, implementation *in vivo* is often limited by immunogenicity. Therefore, nonbiological but precise conjugates, which may be masked from immune systems, are still actively pursued.

Fully synthetic, bottom-up approaches to creating precise multivalent architectures allow for molecular control of stoichiometry and geometry optimized for a specific target. One such example is the submonomer unit assembly of peptoids to form oligomers with monomer chemical functionality in the desired positions. Kirshenbaum and co-workers[59] demonstrated this technique by synthesizing peptoids with precisely 1−6 azide entities in the monomer side chains. From these multivalent constructs, multivalent displays of estradiol were prepared from alkyne-modified steroids. The multivalent constructs were evaluated by a radiometric competitive binding assay. The monovalent peptoid showed ∼6500 weaker affinity than that of the free estradiol, perhaps due to entropic penalties due to immobilization on the scaffold; however, the bivalent conjugate recovered to ∼100-fold weaker affinity. This observation could possibly be attributed to chelate-type binding, as estrogen receptors can exist as dimers. Minor improvements for the tri- and hexavalent conjugates can likely be attributed to effective concentration effects. The solid-phase peptoid synthesis allows for tailoring of space between the active monomers so that the biological structures of interest may be matched. Vidal et al.[98] employed peptoid and porphyrins as small scaffolds to match lectin symmetry. Two lectins with different symmetries were studied. A flexible, linear tetravalent glycol−peptoid conjugates and cyclic peptoids of the same valency were first compared. The linear peptoid did not exhibit any inhibition behavior in a hemagglutination inhibition assay, whereas the cyclic cluster selectively inhibited coagulation with one erythrocyte (*Pseudomonas aeruginosa*) but not the other (*Erythrina cristagalli*) tested. However, there was very little measurable effect of multivalency over the monovalent ligand (∼4 times the potency). By way of contrast, a square planar tetravalent porphyrin selectively inhibited the *Erythrina cristagalli* with over 150 times the relative potency of that of the monovalent glycoside. Increasing the valency to 6 had no additional favorable effect, and changing the symmetry to orient all 4 glycosides in one direction or placing 2 in an opposite direction both negatively impacted the behavior of the conjugate. This study demonstrates the importance of precise control of ligand orientation for minimizing thermodynamic costs in achieving ligand−target interactions, especially with inflexible scaffolds.

The convergent assembly of functionalized dendrons is an interesting strategy to avoid the heterogeneity associated with conjugation to preformed polymer scaffolds, analogous to bottom-up approaches. An approach making use of three independent dendron units was published by Weck and co-workers (Figure 17).[151] In this work, ^{1}H NMR data with molecular-level quantitative integrations are provided to support the structural assignments for the three major base dendron structures (dendrons 1, 2, and 5 in the original report) as well as the key linking step between two of the dendrons. The functionalizable scaffold formed upon linking all three dendrons is designed to have 9 terminal amines and 9 terminal azides on a scaffold that contains a theoretical total of 72

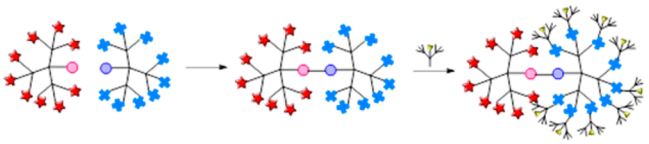

Figure 17. Convergent synthesis of a near-IR dye-functionalized dendrimer.

terminal groups. Again, integrated ^{1}H NMR data provides the primary characterization of this assignment, and integrations are largely in agreement with the assigned structure. Although for divergently synthesized dendrimers such ensemble level data can hide substantial defects in branching structures, in this instance the structural characterization of the individual dendrons used to assemble the final dendrimer gives additional support to the assignment in the larger scaffold. The final functionalization step employed 2 equiv of dye per terminal amine to drive the reaction to completion. MALDI-TOF mass spectrometry indicated that the dendrimer containing 9 dyes was present, although the presence of material resulting from incomplete conversion cannot be ruled out based on the mass spectrometry, NMR, and absorption data presented. In 2010, Weck and co-workers developed a method to construct generation 2 poly(amide)-based dendrons and dendrimer materials using click chemistry. These materials had the multifunctionality of amine, azide, and alkynes.[128] This work represents a large step toward creating monodisperse polymers since the dendrimers synthesized had ~100% completion reactions for each generation, as determined by various characterization techniques. This has been a major challenge in creating many dendrimer materials, including the PAMAM dendrimer.[128] In 2011, Weck and co-workers conjugated these well-defined dendrimer materials to near-infrared cyanine dyes in order to create monodisperse polymer imaging agents.[129]

Assembly of prefunctionalized arms into dendrimer topologies has also been employed to provide better control of ligand-to-scaffold ratio. Improvements using this strategy are illustrated by work out of the Simanek group using the triazine dendrimer scaffold. Their initial efforts employed the statistical, substoichiometric conjugations described in detail above. In order to improve on the distributions obtained, which lead to an undesired level of heterogeneity,[152,153] Simanek et al. constructed a new triazine dendrimer scaffold from prefunctionalized arms nominally containing 16 paclitaxel ligands and 8 PEG chains.[154] A combination of ^{1}H NMR spectroscopy, HPLC, and GPC suggests that the resulting mixture consists of material with the desired 16 and 8 ligand-to-scaffold ratios as well as a second major species, possibly resulting from a missing arm, that contains 14 paclitaxel and 7 PEG.

Convergent approaches are difficult to extend to higher-generation dendrimers. Recent work by Banaszak Holl and co-workers utilized reverse-phase high-performance liquid chromatography (rp-HPLC) to isolate divergent, generation 5 PAMAM dendrimers with precise ligand-to-scaffold ratios.[14,15,83,87] Separation has been achieved using both azide- and alkyne substituted "click" ligands as well as dye ligands. On the semipreparative scale, isolation of tens of milligrams of products is routine. To date, the approaches have been employed for fluorescein and TAMRA dyes,[65] targeting agents,[109] and to assemble dimers, trimers, tetramers, and pentamers of dendrimers (Figure 18).[87] These approaches provide materials with a systematic control of surface hydrophobicity for a given choice of ligand and thus provide an opportunity to explore the impact of ligand-to-dendrimer ratio on opsonization and biodistribution.

FUTURE PERSPECTIVES

In the pursuit of multivalent polymer conjugates that are effective for biomedical applications, many issues must be addressed. First, it is important to acknowledge the conjugation heterogeneity present in a ligand−scaffold conjugate and the impacts of this heterogeneity on the desired application. Then, the best way to minimize or eliminate the impacts of differential hydrophobicity, multivalent binding, and so forth can be determined. Systematic variation of ligand density has proven to be a facile route to improved conjugate activity that can lead to samples that, while still heterogeneous, limit the population of inactive species.[66,117] Such high-average samples, when not

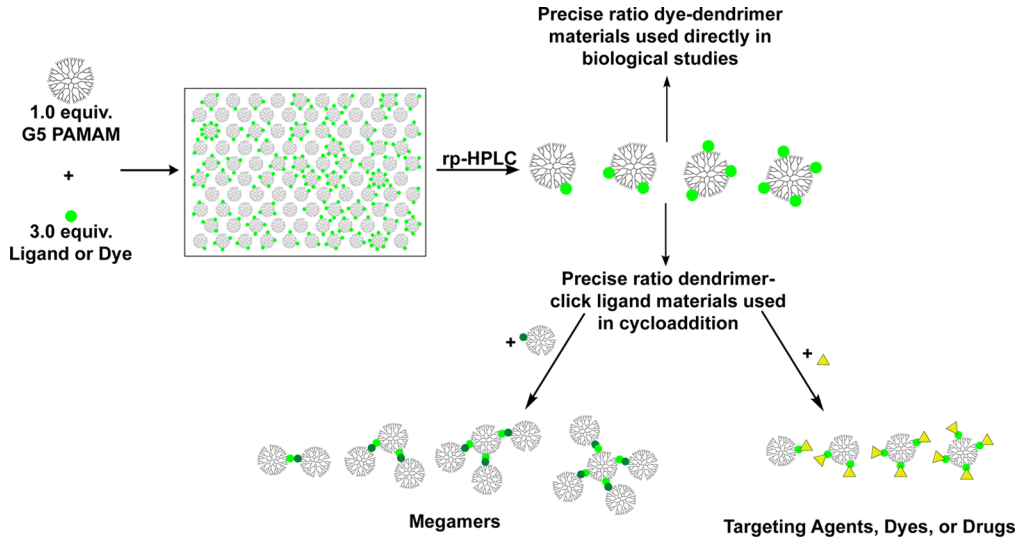

Figure 18. Schematic procedure for obtaining precise ligand-to-dendrimer ratios. rp-HPLC separation of a stochastic mixture of hydrophobic ligands allows isolation of dendrimer containing precise ratio ligand-to-scaffold ratios for dyes and "click" ligands. The click ligands can then be converted to dyes, targeting ligands, or therapeutics.

dx.doi.org/10.1021/bm500921q | *Biomacromolecules* 2014, 15, 3215−3234

plagued with undesired properties such as insolubility or nonspecific cytotoxicity, may be the easiest and/or fastest method to bring a conjugate to clinical scales. The distributions can be further reduced in complexity by the application of heterofunctional ligands.[124] Methods that allow preparation of polymer constructs with a controlled number of functional arms also appear to be particularly promising.[125,133,150,151,154] Achieving precise ligand-to-scaffold ratio for these widely employed multivalent conjugates must also continue as the best way to distinguish mechanisms of activity and identification of active components within a sample.[14,15,65] For other applications, a more structured approach to maximize specific multivalent effects is best for achieving the desired interaction. If target chelation is not a desired outcome (for example, in the PAMAM–folic acid case when even 1 ligand is sufficient to achieve the desired behavior), then it is best to pursue conjugate techniques such as ligand clustering to maximize local concentration effects. Employing flexible scaffolds might also minimize the need for precise control over ligand spatial distributions. If the exact geometry is known, then effort might be best spent in optimization of the scaffold choice for precise control of ligand placement to minimize entropic penalties of bringing multiple ligands into the desired geometry. It is easy to neglect the contribution of effective concentration effects in favor of achieving architectures that exhibit chelate binding in such systems; however, the works highlighted here indicate that these can be the dominant effect. Although much work revolving around clustering has been pursued with glycoclusters, it is reasonable to believe such effects may translate to other ligands of biological interest. An interesting area to pursue would be to combine a precisely tailored geometry, such as that seen with the square planar complexes of Vidal et al., with preclustered ligands on a dendron to high local concentrations and precise localization of cluster geometry.[98] As such, applying ligand clustering via click reaction to either distributed or precise conjugates on flexible scaffolds like PAMAM may provide new optimization of multivalent behavior.

In summary, multivalent, multifunctional polymeric conjugates are highly attractive for the targeted delivery of drugs and imaging agents. However, common approaches to the synthesis of polymer conjugates involve many steps and can lead to complex mixtures and a wide array of products. The presence of these statistically driven product distributions can be hard to assess by most chemical and biological techniques employed to evaluate the samples. As such, progress toward understanding the impact of such heterogeneous distributions on the activity of the conjugates is slow. Recent work in systematically modifying the distributions of ligands present and crafting of precise multivalent architectures has allowed for better elucidation of multivalent behavior.

AUTHOR INFORMATION

Corresponding Author

*E-mail: mbanasza@umich.edu.

Notes

The authors declare no competing financial interest.

ACKNOWLEDGMENTS

The National Cancer Institute (RO1 CA119409) and the National Institute of Biomedical Imaging and Bioengineering (RO1 EB005028) are thanked for their support of our efforts in developing polymer vectors for clinical application.

REFERENCES

(1) Pasut, G.; Veronese, F. M. Polymer–Drug Conjugation, Recent Achievements and General Strategies. *Prog. Polym. Sci.* **2007**, *32*, 933–961.

(2) Duncan, R.; Gaspar, R. Nanomedicine(s) under the Microscope. *Mol. Pharmaceutics* **2011**, *8*, 2101–2141.

(3) Duncan, R.; Richardson, S. C. W. Endocytosis and Intracellular Trafficking as Gateways for Nanomedicine Delivery: Opportunities and Challenges. *Mol. Pharmaceutics* **2012**, *9*, 2380–2402.

(4) Svenson, S. Theranostics: Are We There Yet? *Mol. Pharmaceutics* **2013**, *10*, 848–856.

(5) van der Meel, R.; Vehmeijer, L. J. C.; Kok, R. J.; Storm, G.; van Gaal, E. V. B. Ligand-Targeted Particulate Nanomedicines Undergoing Clinical Evaluation: Current Status. *Adv. Drug Delivery Rev.* **2013**, *65*, 1284–1298.

(6) Röglin, L.; Lempens, E. H. M.; Meijer, E. W. A Synthetic "Tour de Force": Well-Defined Multivalent and Multimodal Dendritic Structures for Biomedical Applications. *Angew. Chem., Int. Ed.* **2011**, *50*, 102–112.

(7) Kelkar, S. S.; Reineke, T. M. Theranostics: Combining Imaging and Therapy. *Bioconjugate Chem.* **2011**, *22*, 1879–1903.

(8) Lee, C. C.; MacKay, J. A.; Fréchet, J. M. J.; Szoka, F. C., Jr. Designing Dendrimers for Biological Applications. *Nat. Biotechnol.* **2005**, *23*, 1517–1526.

(9) Baker, J. R. Why I Believe Nanoparticles Are Crucial as a Carrier for Targeted Drug Delivery. *Wiley Interdiscip. Rev.: Nanomed. Nanobiotechnol.* **2013**, *5*, 423–429.

(10) Boas, U.; Heegaard, P. M. H. Dendrimers in Drug Research. *Chem. Soc. Rev.* **2004**, *33*, 43–63.

(11) Temming, K.; Schiffelers, R. M.; Molema, G.; Kok, R. J. RGD-Based Strategies for Selective Delivery of Therapeutics and Imaging Agents to the Tumour Vasculature. *Drug Resist. Updates* **2005**, *8*, 381–402.

(12) Haag, R.; Kratz, F. Polymer Therapeutics: Concepts and Applications. *Angew. Chem., Int. Ed.* **2006**, *45*, 1198–1215.

(13) Ringsdorf, H. Structure and Properties of Pharmacologically Active Polymers. *J. Polym. Sci., Part C: Polym. Symp.* **1975**, *51*, 135–153.

(14) Mullen, D. G.; Banaszak Holl, M. M. Heterogeneous Ligand–Nanoparticle Distributions: A Major Obstacle to Scientific Understanding and Commercial Translation. *Acc. Chem. Res.* **2011**, *44*, 1135–1145.

(15) Mullen, D. G.; Fang, M.; Desai, A.; Baker, J. R., Jr.; Orr, B. G.; Banaszak Holl, M. M. A Quantitative Assessment of Nanoparticle–Ligand Distributions: Implications for Targeted Drug and Imaging Delivery in Dendrimer Conjugates. *ACS Nano* **2010**, *4*, 657–670.

(16) McNeil, S. E. *Characterization of Nanoparticles Intended for Drug Delivery*; Humana Press: Totowa, NJ, 2011; Vol. *697*.

(17) Wacker, M. G. Nanotherapeutics – Product Development Along the "Nanomaterial" Discussion. *J. Pharm. Sci.* **2014**, *103*, 777–784.

(18) Barenholz, Y. Doxil – The First FDA-Approved Nano-Drug: Lessons Learned. *J. Controlled Release* **2012**, *160*, 117–134.

(19) Davis, M. E. The First Targeted Delivery of siRNA in Humans via a Self-Assembling, Cyclodextrin Polymer-Based Nanoparticle: From Concept to Clinic. *Mol. Pharmaceutics* **2009**, *6*, 659–668.

(20) Wacker, M. Nanocarriers for Intravenous Injection—The Long Hard Road to the Market. *Int. J. Pharm.* **2013**, *457*, 50–62.

(21) Petros, R. A.; DeSimone, J. M. Strategies in the Design of Nanoparticles for Therapeutic Applications. *Nat. Rev. Drug Discovery* **2010**, *9*, 615–627.

(22) Filpula, D.; Zhao, H. Releasable PEGylation of Proteins with Customized Linkers. *Adv. Drug Delivery Rev.* **2008**, *60*, 29–49.

(23) Larson, N.; Ghandehari, H. Polymeric Conjugates for Drug Delivery. *Chem. Mater.* **2012**, *24*, 840–853.

(24) Abuchowski, A.; McCoy, J. R.; Palczuk, N. C.; Vanes, T.; Davis, F. F. Effect of Covalent Attachment of Polyethylene-Glycol on Immunogenicity and Circulating Life of Bovine Liver Catalase. *J. Biol. Chem.* **1977**, *252*, 3582−3586.
(25) Abuchowski, A.; Vanes, T.; Palczuk, N. C.; Davis, F. F. Alteration of Immunological Properties of Bovine Serum-Albumin by Covalent Attachment of Polyethylene-Glycol. *J. Biol. Chem.* **1977**, *252*, 3578−3581.
(26) Hrkach, J.; Von Hoff, D.; Ali, M. M.; Andrianova, E.; Auer, J.; Campbell, T.; De Witt, D.; Figa, M.; Figueiredo, M.; Horhota, A.; Low, S.; McDonnell, K.; Peeke, E.; Retnarajan, B.; Sabnis, A.; Schnipper, E.; Song, J. J.; Song, Y. H.; Summa, J.; Tompsett, D.; Troiano, G.; Van Geen Hoven, T.; Wright, J.; LoRusso, P.; Kantoff, P. W.; Bander, N. H.; Sweeney, C.; Farokhzad, O. C.; Langer, R.; Zale, S. Preclinical Development and Clinical Translation of a PSMA-Targeted Docetaxel Nanoparticle with a Differentiated Pharmacological Profile. *Sci. Trans. Med.* **2012**, *4*, 128−139.
(27) Gu, F.; Zhang, L.; Teply, B. A.; Mann, N.; Wang, A.; Radovic-Moreno, A. F.; Langer, R.; Farokhzad, O. C. Precise Engineering of Targeted Nanoparticles by Using Self-Assembled Biointegrated Block Copolymers. *Proc. Natl. Acad. Sci. U.S.A.* **2008**, *105*, 2586−2591.
(28) Goniewicz, M. L.; Delijewski, M. Nicotine Vaccines to Treat Tobacco Dependence. *Hum. Vaccines Immunother.* **2013**, *9*, 19−31.
(29) Janib, S. M.; Moses, A. S.; MacKay, J. A. Imaging and Drug Delivery Using Theranostic Nanoparticles. *Adv. Drug Delivery Rev.* **2010**, *62*, 1052−1063.
(30) Xie, J.; Lee, S.; Chen, X. Nanoparticle-Based Theranostic Agents. *Adv. Drug Delivery Rev.* **2010**, *62*, 1064−1079.
(31) Kukowska-Latallo, J. F.; Candido, K. A.; Cao, Z.; Nigavekar, S. S.; Majoros, I. J.; Thomas, T. P.; Balogh, L. P.; Khan, M. K.; Baker, J. R. Nanoparticle Targeting of Anticancer Drug Improves Therapeutic Response in Animal Model of Human Epithelial Cancer. *Cancer Res.* **2005**, *65*, 5317−5324.
(32) Choi, S. K.; Myc, A.; Silpe, J. E.; Sumit, M.; Wong, P. T.; McCarthy, K.; Desai, A. M.; Thomas, T. P.; Kotlyar, A.; Holl, M. M. B.; Orr, B. G.; Baker, J. R. Dendrimer-Based Multivalent Vancomycin Nanoplatform for Targeting the Drug-Resistant Bacterial Surface. *ACS Nano* **2012**, *7*, 214−228.
(33) Le Droumaguet, B.; Nicolas, J.; Brambilla, D.; Mura, S.; Maksimenko, A.; De Kimpe, L.; Salvati, E.; Zona, C.; Airoldi, C.; Canovi, M.; Gobbi, M.; Magali, N.; La Ferla, B.; Nicotra, F.; Scheper, W.; Flores, O.; Masserini, M.; Andrieux, K.; Couvreur, P. Versatile and Efficient Targeting Using a Single Nanoparticulate Platform: Application to Cancer and Alzheimer's Disease. *ACS Nano* **2012**, *6*, 5866−5879.
(34) Shamay, Y.; Adar, L.; Ashkenasy, G.; David, A. Light Induced Drug Delivery into Cancer Cells. *Biomaterials* **2011**, *32*, 1377−1386.
(35) Tansey, W.; Ke, S.; Cao, X. Y.; Pasuelo, M. J.; Wallace, S.; Li, C. Synthesis and Characterization of Branched Poly(L-glutamic acid) as a Biodegradable Drug Carrier. *J. Controlled Release* **2004**, *94*, 39−51.
(36) Wang, J.; Liu, W.; Tu, Q.; Wang, J.; Song, N.; Zhang, Y.; Nie, N.; Wang, J. Folate-Decorated Hybrid Polymeric Nanoparticles for Chemically and Physically Combined Paclitaxel Loading and Targeted Delivery. *Biomacromolecules* **2010**, *12*, 228−234.
(37) Sharma, A.; Soliman, G. M.; Al-Hajaj, N.; Sharma, R.; Maysinger, D.; Kakkar, A. Design and Evaluation of Multifunctional Nanocarriers for Selective Delivery of Coenzyme Q10 to Mitochondria. *Biomacromolecules* **2011**, *13*, 239−252.
(38) Chandna, P.; Saad, M.; Wang, Y.; Ber, E.; Khandare, J.; Vetcher, A. A.; Soldatenkov, V. A.; Minko, T. Targeted Proapoptotic Anticancer Drug Delivery System. *Mol. Pharmaceutics* **2007**, *4*, 668−678.
(39) Saad, M.; Garbuzenko, O. B.; Ber, E.; Chandna, P.; Khandare, J. J.; Pozharov, V. P.; Minko, T. Receptor Targeted Polymers, Dendrimers, Liposomes: Which Nanocarrier Is the Most Efficient for Tumor-Specific Treatment and Imaging? *J. Controlled Release* **2008**, *130*, 107−114.
(40) Santra, S.; Kaittanis, C.; Perez, J. M. Cytochrome c Encapsulating Theranostic Nanoparticles: A Novel Bifunctional System for Targeted Delivery of Therapeutic Membrane-Impermeable Proteins to Tumors and Imaging of Cancer Therapy. *Mol. Pharmaceutics* **2010**, *7*, 1209−1222.
(41) Fréchet, J. M. J.; Lochman, L.; Smigol, V.; Svec, F. Reversed-Phase High-Performance Liquid Chromatography of Functionalized Dendritic Macromolecules. *J. Chromatogr. A* **1994**, *667*, 284−289.
(42) Hawker, C. J.; Fréchet, J. M. J. Preparation of Polymers with Controlled Molecular Architecture. A New Convergent Approach to Dendritic Macromolecules. *J. Am. Chem. Soc.* **1990**, *112*, 7638−7647.
(43) Grayson, S. M.; Fréchet, J. M. J. Convergent Dendrons and Dendrimers: From Synthesis to Applications. *Chem. Rev.* **2001**, *101*, 3819−3868.
(44) Hawker, C. J.; Fréchet, J. M. J. A New Convergent Approach To Monodisperse Dendritic Macromolecules. *J. Chem. Soc. Chem. Comm.* **1990**, 1010−1013.
(45) Tomalia, D. A.; Baker, H.; Dewald, J.; Hall, M.; Kallos, G.; Martin, S.; Roeck, J.; Ryder, J.; Smith, P. A New Class of Polymers: Starburst-Dendritic Macromolecules. *Polym. Chem.* **1985**, *17*, 117−132.
(46) Esfand, R.; Tomalia, D. A. Poly(amidoamine) (PAMAM) Dendrimers: From Biomimicry to Drug Delivery and Biomedical Applications. *Drug Discovery Today* **2001**, *6*, 427−436.
(47) Tomalia, D. A. Dendrimers as Multi-Purpose Nanodevices for Oncology Drug Delivery and Diagnostic Imaging. *J. Nanomed. Nanotechnol.* **2006**, *2*, 309.
(48) Menjoge, A. R.; Kannan, R. M.; Tomalia, D. A. Dendrimer-Based Drug and Imaging Conjugates: Design Considerations for Nanomedical Applications. *Drug Discovery Today* **2010**, *15*, 171−185.
(49) Newkome, G. R.; Baker, G. R.; Arai, S.; Saunders, M. J.; Russo, P. S.; Theriot, K. J.; Moorefield, C. N.; Rogers, L. E.; Miller, J. E. Cascade Molecules. Part 6. Synthesis and Characterization of Two-Directional Cascade Molecules and Formation of Aqueous Gels. *J. Am. Chem. Soc.* **1990**, *112*, 8458−8465.
(50) Newkome, G. R.; He, E.; Moorefield, C. N. Suprasupermolecules with Novel Properties: Metallodendrimers. *Chem. Rev.* **1999**, *99*, 1689−1746.
(51) Newkome, G. R.; Shreiner, C. D. Poly(amidoamine), Polypropylenimine, And Related Dendrimers and Dendrons Possessing Different 1 → 2 Branching Motifs: An Overview of the Divergent Procedures. *Polymer* **2008**, *49*, 1−173.
(52) Archut, A.; Vögtle, F. Functional Cascade Molecules. *Chem. Soc. Rev.* **1998**, *27*, 233−240.
(53) Fischer, M.; Vögtle, F. Dendrimers: From Design to Application—A Progress Report. *Angew. Chem., Int. Ed.* **1999**, *38*, 884−905.
(54) Vögtle, F.; Gestermann, S.; Hesse, R.; Schwierz, H.; Windisch, B. Functional Dendrimers. *Prog. Polym. Sci.* **2000**, *25*, 987−1041.
(55) Walter, M. V.; Malkoch, M. Simplifying the Synthesis of Dendrimers: Accelerated Approaches. *Chem. Soc. Rev.* **2012**, *41*, 4593−4609.
(56) Fournier, D.; Hoogenboom, R.; Schubert, U. S. Clicking Polymers: A Straightforward Approach to Novel Macromolecular Architectures. *Chem. Soc. Rev.* **2007**, *36*, 1369−1380.
(57) Ihre, H.; Hult, A.; Fréchet, J. M. J.; Gitsov, I. Double-Stage Convergent Approach for the Synthesis of Functionalized Dendritic Aliphatic Polyesters Based on 2,2-Bis(hydroxymethyl)propionic Acid. *Macromolecules* **1998**, *31*, 4061−4068.
(58) Burai, R.; Chatwichien, J.; McNaughton, B. R. A Programmable "Build-Couple" Approach to the Synthesis of Heterofunctionalized Polyvalent Molecules. *Org. Biomol. Chem.* **2011**, *9*, 5056−5058.
(59) Holub, J. M.; Garabedian, M. J.; Kirshenbaum, K. Peptoids on Steroids: Precise Multivalent Estradiol−Peptidomimetic Conjugates Generated via Azide−Alkyne [3 + 2] Cycloaddition Reactions. *QSAR Comb. Sci.* **2007**, *26*, 1175−1180.
(60) Tomalia, D. A.; Christensen, J. B.; Boas, U. The Dendritic State. In *Dendrimers, Dendrons and Dendritic Polymers: Discovery, Applications, the Future*; Cambridge University Press: Cambridge, 2012; pp 2−32.
(61) Christensen, J. B.; Tomalia, D. A. Dendrimers as Quantized Nano-modules in the Nanotechnology Field. In *Designing Dendrimers.*

Campagna, S., Ceroni, P., Puntoriero, F., Eds.; J. Wiley & Sons: Hoboken, NJ, 2012; pp 1−33.
(62) Mullen, D. G.; Borgmeier, E. L.; Fang, M.; McNerny, D. Q.; Desai, A.; Baker, J. R.; Orr, B. G.; Banaszak Holl, M. M. Effect of Mass Transport in the Synthesis of Partially Acetylated Dendrimer: Implications for Functional Ligand−Nanoparticle Distributions. *Macromolecules* **2010**, *43*, 6577−6587.
(63) Hakem, I. F.; Leech, A. M.; Johnson, J. D.; Donahue, S. J.; Walker, J. P.; Bockstaller, M. R. Understanding Ligand Distributions in Modified Particle and Particlelike Systems. *J. Am. Chem. Soc.* **2010**, *132*, 16593−16598.
(64) Hakem, I. F.; Leech, A. M.; Bohn, J.; Walker, J. P.; Bockstaller, M. R. Analysis of Heterogeneity in Nonspecific PEGylation Reactions of Biomolecules. *Biopolymers* **2013**, *99*, 427−435.
(65) Dougherty, C. A.; Furgal, J. C.; van Dongen, M. A.; Goodson, T., III; Banaszak Holl, M. M. Isolation and Characterization of Precise Dye/Dendrimer Ratios. *Chem.—Eur. J.* **2014**, *20*, 4638−4645.
(66) Wängler, C.; Moldenhauer, G.; Saffrich, R.; Knapp, E. M.; Beijer, B.; Schnölzer, M.; Wängler, B.; Eisenhut, M.; Haberkorn, U.; Mier, W. PAMAM Structure-Based Multifunctional Fluorescent Conjugates for Improved Fluorescent Labelling of Biomacromolecules. *Chem.—Eur. J.* **2008**, *14*, 8116−8130.
(67) Yang, H.; Kao, W. J. Dendrimers for Pharmaceutical and Biomedical Applications. *J. Biomater. Sci., Polym. Ed.* **2006**, *17*, 3−19.
(68) Kopeček, J. Reactive Copolymers of N-(2-Hydroxypropyl)-Methacrylamide with N-Methacryloylated Derivatives of L-Leucine and L-Phenylalanine, 1. Preparation, Characterization, and Reactions with Diamines. *Makromol. Chem.* **1977**, *178*, 2169−2183.
(69) Kopeček, J.; Kopečková, P. HPMA Copolymers: Origins, Early Developments, Present, and Future. *Adv. Drug Delivery Rev.* **2010**, *62*, 122−149.
(70) Rihova, B.; Bilej, M.; Vetvicka, V.; Ulbrich, K.; Strohalm, J.; Kopecek, J.; Duncan, R. Biocompatibility of N-(2-Hydroxypropyl) Methacrylamide Copolymers Containing Adriamycin: Immunogenicity, and Effect on Haematopoietic Stem Cells in Bone Marrow *in Vivo* and Mouse Splenocytes and Human Peripheral Blood Lymphocytes *in Vitro*. *Biomaterials* **1989**, *10*, 335−342.
(71) Vasey, P. A.; Kaye, S. B.; Morrison, R.; Twelves, C.; Wilson, P.; Duncan, R.; Thomson, A. H.; Murray, L. S.; Hilditch, T. E.; Murray, T.; Burtles, S.; Fraier, D.; Frigerio, E.; Cassidy, J. Phase I Clinical and Pharmacokinetic Study of PK1 [N-(2-Hydroxypropyl)methacrylamide Copolymer Doxorubicin]: First Member of a New Class of Chemotherapeutic Agents—Drug−Polymer Conjugates. *Clin. Cancer Res.* **1999**, *5*, 83−94.
(72) Teodorescu, M.; Matyjaszewski, K. Atom Transfer Radical Polymerization of (Meth)acrylamides. *Macromolecules* **1999**, *32*, 4826−4831.
(73) Scales, C. W.; Vasilieva, Y. A.; Convertine, A. J.; Lowe, A. B.; McCormick, C. L. Direct, Controlled Synthesis of the Non-immunogenic, Hydrophilic Polymer, Poly(N-(2-hydroxypropyl)-methacrylamide) via RAFT in Aqueous Media. *Biomacromolecules* **2005**, *6*, 1846−1850.
(74) Yu, Y.; Chen, C. K.; Law, W. C.; Mok, J.; Zou, J.; Prasad, P. N.; Cheng, C. Well-Defined Degradable Brush Polymer-Drug Conjugates for Sustained Delivery of Paclitaxel. *Mol. Pharmaceutics* **2013**, *10*, 867−874.
(75) Lee, C. C.; Gillies, E. R.; Fox, M. E.; Guillaudeu, S. J.; Fréchet, J. M. J.; Dy, E. E.; Szoka, F. C. A Single Dose of Doxorubicin-Functionalized Bow-Tie Dendrimer Cures Mice Bearing C-26 Colon Carcinomas. *Proc. Natl. Acad. Sci. U.S.A.* **1996**, *103*, 16649−16654.
(76) Goonewardena, S. N.; Kratz, J. D.; Zong, H.; Desai, A. M.; Tang, S.; Emery, S.; Baker, J. R.; Huang, B. Design Considerations for PAMAM Dendrimer Therapeutics. *Bioorg. Med. Chem. Lett.* **2013**, *23*, 2872−2875.
(77) Patri, A.; Kukowskalatallo, J.; Baker, J. R., Jr. Targeted Drug Delivery with Dendrimers: Comparison of the Release Kinetics of Covalently Conjugated Drug and Non-Covalent Drug Inclusion Complex. *Adv. Drug Delivery Rev.* **2005**, *57*, 2203−2214.
(78) Kannan, S.; Dai, H.; Navath, R. S.; Balakrishnan, B.; Jyoti, A.; Janisse, J.; Romero, R.; Kannan, R. M. Dendrimer-Based Postnatal Therapy for Neuroinflammation and Cerebral Palsy in a Rabbit Model. *Sci. Trans. Med.* **2012**, *4*, 130ra146.
(79) Thomas, T. P.; Huang, B.; Choi, S. K.; Silpe, J. E.; Kotlyar, A.; Desai, A. M.; Zong, H.; Gam, J.; Joice, M.; Baker, J. R. Polyvalent Dendrimer-Methotrexate as a Folate Receptor-Targeted Cancer Therapeutic. *Mol. Pharmaceutics* **2012**, *9*, 2669−2676.
(80) Boyd, B. J.; Kaminskas, L. M.; Karellas, P.; Krippner, G.; Lessene, R.; Porter, C. J. H. Cationic Poly-L-lysine Dendrimers: Pharmacokinetics, Biodistribution, and Evidence for Metabolism and Bioresorption after Intravenous Administration to Rats. *Mol. Pharmaceutics* **2006**, *3*, 614−627.
(81) Kaminskas, L. M.; Boyd, B. J.; Karellas, P.; Henderson, S. A.; Giannis, M. P.; Krippner, G. Y.; Porter, C. J. H. Impact of Surface Derivatization of Poly-L-lysine Dendrimers with Anionic Aryisulfonate or Succinate Groups on Intravenous Pharmacokinetics and Disposition. *Mol. Pharmaceutics* **2007**, *4*, 949−961.
(82) Tyssen, D.; Henderson, S. A.; Johnson, A.; Sterjovski, J.; Moore, K.; La, J.; Zanin, M.; Sonza, S.; Karellas, P.; Giannis, M. P.; Krippner, G.; Wesselingh, S.; McCarthy, T.; Gorry, P. R.; Ramsland, P. A.; Cone, R.; Paull, J. R. A.; Lewis, G. R.; Tachedjian, G. Structure Activity Relationship of Dendrimer Microbicides with Dual Action Antiviral Activity. *PLoS One* **2010**, *5*, e12309.
(83) Mullen, D. G.; Borgmeier, E. L.; Desai, A. M.; van Dongen, M. A.; Barash, M.; Cheng, X.-m.; Baker, J. R.; Banaszak Holl, M. M. Isolation and Characterization of Dendrimers with Precise Numbers of Functional Groups. *Chem.—Eur. J.* **2010**, *16*, 10675−10678.
(84) Casanova, D.; Giaume, D.; Moreau, M.; Martin, J.-L.; Gacoin, T.; Boilot, J.-P.; Alexandrou, A. Counting the Number of Proteins Coupled to Single Nanoparticles. *J. Am. Chem. Soc.* **2007**, *129*, 12592−12593.
(85) Mullen, D. G.; Desai, A.; van Dongen, M. A.; Barash, M.; Baker, J. R., Jr.; Banaszak Holl, M. M. Best Practices for Purification and Characterization of PAMAM Dendrimer. *Macromolecules* **2012**, *45*, 5316−5320.
(86) van Dongen, M. A.; Desai, A.; Orr, B. G.; Baker, J. R., Jr.; Banaszak Holl, M. M. Quantitative Analysis of Generation and Branch Defects in G5 Poly(amidoamine) Dendrimer. *Polymer.* **2013**, *54*, 4126−4133.
(87) van Dongen, M. A.; Vaidyanathan, S.; Banaszak Holl, M. M. PAMAM Dendrimers as Quantized Building Blocks for Novel Nanostructures. *Soft Matter* **2013**, *9*, 11188−11196.
(88) Mullen, D. G.; Desai, A. M.; Waddell, J. N.; Cheng, X.-M.; Kelly, C. V.; McNerny, D. Q.; Majoros, I. n. J.; Baker, J. R.; Sander, L. M.; Orr, B. G.; Banaszak Holl, M. M. The Implications of Stochastic Synthesis for the Conjugation of Functional Groups to Nanoparticles. *Bioconjugate Chem.* **2008**, *19*, 1748−1752.
(89) Lo, S.-T.; Stern, S.; Clogston, J. D.; Zheng, J.; Adiseshaiah, P. P.; Dobrovolskaia, M.; Lim, J.; Patri, A. K.; Sun, X.; Simanek, E. E. Biological Assessment of Triazine Dendrimer: Toxicological Profiles, Solution Behavior, Biodistribution, Drug Release and Efficacy in a PEGylated, Paclitaxel Construct. *Mol. Pharmaceutics* **2010**, *7*, 993−1006.
(90) Krishnamurthy, V. M.; Estroff, L. A.; Whitesides, G. M. Multivalency in Ligand Design. In *Fragment-Based Approaches in Drug Discovery*; Jahnke, W., Erlanson, D. A., Eds.; Wiley-VCH: Weinheim, Germany, 2006; pp 11−53.
(91) Chittasupho, C. Multivalent Ligand: Design Principle for Targeted Therapeutic Delivery Approach. *Ther. Delivery* **2012**, *3*, 1171−1187.
(92) Levine, P. M.; Carberry, T. P.; Holub, J. M.; Kirshenbaum, K. Crafting Precise Multivalent Architectures. *MedChemComm.* **2013**, *4*, 493−509.
(93) Rolland, O.; Turrin, C.-O.; Caminade, A.-M.; Majoral, J.-P. Dendrimers and Nanomedicine: Multivalency in Action. *New J. Chem.* **2009**, *33*, 1809−1824.

(94) Barnard, A.; Smith, D. K. Self-Assembled Multivalency: Dynamic Ligand Arrays for High-Affinity Binding. *Angew. Chem., Int. Ed.* **2012**, *51*, 6572−6581.
(95) Mann, D. A.; Kanai, M.; Maly, D. J.; Kiessling, L. L. Probing Low Affinity and Multivalent Interactions with Surface Plasmon Resonance: Ligands for Concanavalin A. *J. Am. Chem. Soc.* **1998**, *120*, 10575−10582.
(96) Hong, S.; Leroueil, P. R.; Majoros, I. J.; Orr, B. G.; Baker, J. R.; Banaszak Holl, M. M. The Binding Avidity of a Nanoparticle-Based Multivalent Targeted Drug Delivery Platform. *Chem. Biol.* **2007**, *14*, 107−115.
(97) Nijhuis, C. A.; Yu, F.; Knoll, W.; Huskens, J.; Reinhoudt, D. N. Multivalent Dendrimers at Molecular Printboards: Influence of Dendrimer Structure on Binding Strength and Stoichiometry and Their Electrochemically Induced Desorption. *Langmuir* **2005**, *21*, 7866−7876.
(98) Cecioni, S.; Faure, S.; Darbost, U.; Bonnamour, I.; Parrot-Lopez, H.; Roy, O.; Taillefumier, C.; Wimmerová, M.; Praly, J.-P.; Imberty, A.; Vidal, S. Selectivity among Two Lectins: Probing the Effect of Topology, Multivalency and Flexibility of "Clicked" Multivalent Glycoclusters. *Chem.—Eur. J.* **2011**, *17*, 2146−2159.
(99) Dam, T. K.; Brewer, C. F. Thermodynamic Studies of Lectin−Carbohydrate Interactions by Isothermal Titration Calorimetry. *Chem. Rev.* **2002**, *102*, 387−430.
(100) Silpe, J. E.; Sumit, M.; Huang, B.; Kotlyar, A.; van Dongen, M. A.; Banaszak Holl, M. M.; Orr, B. G.; Choi, S. K. Avidity Modulation of Folate-Targeted Multivalent Dendrimers for Evaluating Biophysical Models of Cancer Targeting Nanoparticles. *ACS Chem. Biol.* **2013**, *8*, 2063−2071.
(101) Nakagawa, O.; Ming, X.; Huang, L.; Juliano, R. L. Targeted Intracellular Delivery of Antisense Oligonucleotides via Conjugation with Small-Molecule Ligands. *J. Am. Chem. Soc.* **2010**, *132*, 8848−8849.
(102) Zhou, Q.-H.; You, Y.-Z.; Wu, C.; Huang, Y.; Oupický, D. Cyclic RGD-Targeting of Reversibly Stabilized DNA Nanoparticles Enhances Cell Uptake and Transfection *in Vitro*. *J. Drug Targeting* **2009**, *17*, 364−373.
(103) Reuter, J. D.; Myc, A.; Hayes, M. M.; Gan, Z.; Roy, R.; Qin, D.; Yin, R.; Piehler, L. T.; Esfand, R.; Tomalia, D. A.; Baker, J. R. Inhibition of Viral Adhesion and Infection by Sialic-Acid-Conjugated Dendritic Polymers. *Bioconjugate Chem.* **1999**, *10*, 271−278.
(104) Munoz, E. M.; Correa, J.; Fernandez-Megia, E.; Riguera, R. Probing the Relevance of Lectin Clustering for the Reliable Evaluation of Multivalent Carbohydrate Recognition. *J. Am. Chem. Soc.* **2009**, *131*, 17765−17767.
(105) Gómez-García, M.; Benito, J. M.; Butera, A. P.; Mellet, C. O.; Fernández, J. M. G.; Blanco, J. L. J. Probing Carbohydrate-Lectin Recognition in Heterogeneous Environments with Monodisperse Cyclodextrin-Based Glycoclusters. *J. Org. Chem.* **2011**, *77*, 1273−1288.
(106) Bossu, I.; Sulc, M.; Krenek, K.; Dufour, E.; Garcia, J.; Berthet, N.; Dumy, P.; Kren, V.; Renaudet, O. Dendri-RAFTs: A Second Generation of Cyclopeptide-Based Glycoclusters. *Org. Biomol. Chem.* **2011**, *9*, 1948−1959.
(107) Waddell, J. N.; Mullen, D. G.; Orr, B. G.; Banaszak Holl, M. M.; Sander, L. M. Origin of Broad Polydispersion in Functionalized Dendrimers and Its Effects on Cancer-Cell Binding Affinity. *Phys. Rev. E* **2010**, *82*, 036108.
(108) Licata, N. A.; Tkachenko, A. V. Kinetic Limitations of Cooperativity-Based Drug Delivery Systems. *Phys. Rev. Lett.* **2008**, *100*, 158102.
(109) van Dongen, M. A.; Silpe, J. E.; Dougherty, C.; Kanduluru, A. K.; Choi, S. K.; Orr, B. G.; Low, P. S.; Banaszak Holl, M. M. Avidity Mechanism of Dendrimer-Folic Acid Conjugates. *Mol. Pharmaceutics* **2014**, *11*, 1696−1706.
(110) Martinez-Veracoechea, F. J.; Frenkel, D. Designing Super Selectivity in Multivalent Nano-Particle Binding. *Proc. Natl. Acad. Sci. U.S.A.* **2011**, *108*, 10963−10968.
(111) Duan, X.; Li, Y. Physicochemical Characteristics of Nanoparticles Affect Circulation, Biodistribution, Cellular Internalization, and Trafficking. *Small* **2013**, *9*, 1521−1532.
(112) Alexis, F.; Pridgen, E.; Molnar, L. K.; Farokhzad, O. C. Factors Affecting the Clearance and Biodistribution of Polymeric Nanoparticles. *Mol. Pharmaceutics* **2008**, *5*, 505−515.
(113) Moyano, D. F.; Goldsmith, M.; Solfiell, D. J.; Landesman-Milo, D.; Miranda, O. R.; Peer, D.; Rotello, V. M. Nanoparticle Hydrophobicity Dictates Immune Response. *J. Am. Chem. Soc.* **2012**, *134*, 3965−3967.
(114) Wang, J.; Tian, S.; Petros, R. A.; Napier, M. E.; DeSimone, J. M. The Complex Role of Multivalency in Nanoparticles Targeting the Transferrin Receptor for Cancer Therapies. *J. Am. Chem. Soc.* **2010**, *132*, 11306−11313.
(115) Chen, M.; Yin, M. Design and Development of Fluorescent Nanostructures for Bioimaging. *Prog. Polym. Sci.* **2014**, *39*, 365−395.
(116) Duhamel, J. Global Analysis of Fluoresence Decays to Probe the Internal Dynamics of Fluorescently Labeled Macromolecules. *Langmuir* **2014**, *30*, 2307−2324.
(117) Kim, Y.; Kim, S. H.; Tanyeri, M.; Katzenellenbogen, J. A.; Schroeder, C. M. Dendrimer Probes for Enhanced Photostability and Localization in Fluorescence Imaging. *Biophys. J.* **2013**, *104*, 1566−1575.
(118) Opitz, A. W.; Czymmek, K. J.; Wickstrom, E.; Wagner, N. J. Uptake, Effux, And Mass Transfer Coefficient of Fluorescent PAMAM Dendrimers into Pancreatic Cancer Cells. *Biochem. Biophys. Acta.* **2013**, *1828*, 294−301.
(119) Srinivas, O.; Radhika, S.; Bandaru, N. M.; Nadimpalli, S. K.; Jayaraman, N. Synthesis and Biological Evaluation of Mannose-6-phosphate-Coated Multivalent Dendritic Cluster Glycosides. *Org. Biomol. Chem.* **2005**, *3*, 4252−4257.
(120) Welsh, D. J.; Smith, D. K. Comparing Dendritic and Self-Assembly Strategies to Multivalency-RGD Peptide−Integrin Interactions. *Org. Biomol. Chem.* **2011**, *9*, 4795−4801.
(121) Carberry, T. P.; Tarallo, R.; Falanga, A.; Finamore, E.; Galdiero, M.; Weck, M.; Galdiero, S. Dendrimer Functionalization with a Membrane-Interacting Domain of Herpes Simplex Virus Type 1: Towards Intracellular Delivery. *Chem.—Eur. J.* **2012**, *18*, 13678−13685.
(122) Martin, A. L.; Li, B.; Gillies, E. R. Surface Functionalization of Nanomaterials with Dendritic Groups: Toward Enhanced Binding to Biological Targets. *J. Am. Chem. Soc.* **2008**, *131*, 734−741.
(123) Wang, Y.; Wang, Y.; Breed, D. R.; Manoharan, V. N.; Feng, L.; Hollingsworth, A. D.; Weck, M.; Pine, D. J. Colloids with Valence and Specific Directional Bonding. *Nature* **2012**, *491*, 51−55.
(124) Zong, H.; Thomas, T. P.; Lee, K.-H.; Desai, A. M.; Li, M.-h.; Kotlyar, A.; Zhang, Y.; Leroueil, P. R.; Gam, J. J.; Banaszak Holl, M. M.; Baker, J. R. Bifunctional PAMAM Dendrimer Conjugates of Folic Acid and Methotrexate with Defined Ratio. *Biomacromolecules* **2012**, *13*, 982−991.
(125) Luo, H.; Yang, J.; Jin, H.; Huang, C.; Fu, J.; Yang, F.; Gong, H.; Zeng, S.; Luo, Q.; Zhang, Z. Tetrameric far-red fluorescent protein as a scaffold to assemble an octavalent peptide nanoprobe for enhanced tumor targeting and intracellular uptake in vivo. *FASEB J.* **2011**, *25*, 1865−1873.
(126) Kostiainen, M. A.; Szilvay, G. R.; Lehtinen, J.; Smith, D. K.; Linder, M. B.; Urtti, A.; Ikkala, O. Precisely Defined Protein−Polymer Conjugates: Construction of Synthetic DNA Binding Domains on Proteins by Using Multivalent Dendrons. *ACS Nano* **2007**, *1*, 103−113.
(127) Axup, J. Y.; Bajjuri, K. M.; Ritland, M.; Hutchins, B. M.; Kim, C. H.; Kazane, S. A.; Halder, R.; Forsyth, J. S.; Santidrian, A. F.; Stafin, K.; Lu, Y.; Tran, H.; Seller, A. J.; Biroc, S. L.; Szydlik, A.; Pinkstaff, J. K.; Tian, F.; Sinha, S. C.; Felding-Habermann, B.; Smider, V. V.; Schultz, P. G. Synthesis of Site-Specific Antibody−Drug Conjugates Using Unnatural Amino Acids. *Proc. Nat. Acad. Sci. U.S.A.* **2012**, *109*, 16101−16106.
(128) Ornelas, C.; Broichhagen, J.; Weck, M. Strain-Promoted Alkyne Azide Cycloaddition for the Functionalization of Poly(amide)-

Based Dendrons and Dendrimers. *J. Am. Chem. Soc.* **2010**, *132*, 3923−3931.
(129) Ornelas, C.; Lodescar, R.; Durandin, A.; Canary, J. W.; Pennell, R.; Liebes, L. F.; Weck, M. Combining Aminocyanine Dyes with Polyamide Dendrons: A Promising Strategy for Imaging in the Near-Infrared Region. *Chem.—Eur. J.* **2011**, *17*, 3619−3629.
(130) Ryan, G. M.; Kaminskas, L. M.; Kelly, B. D.; Owen, D. J.; McIntosh, M. P.; Porter, C. J. H. Pulmonary Administration of PEGylated Polylysine Dendrimers: Absorption from the Lung versus Retention within the Lung Is Highly Size-Dependent. *Mol. Pharmaceutics* **2013**, *10*, 2986−2995.
(131) Kaminskas, L. M.; Kelly, B. D.; McLeod, V. M.; Boyd, B. J.; Krippner, G. Y.; Williams, E. D.; Porter, C. J. H. Pharmacokinetics and Tumor Disposition of PEGylated, Methotrexate Conjugated Poly-L-lysine Dendrimers. *Mol. Pharmaceutics* **2009**, *6*, 1190−1204.
(132) Kaminskas, L. M.; McLeod, V. M.; Ryan, G. M.; Kelly, B. D.; Haynes, J. M.; Williamson, M.; Thienthong, N.; Owen, D. J.; Porter, C. J. H. Pulmonary Administration of a Doxorubicin-Conjugated Dendrimer Enhances Drug Exposure to Lung Metastases and Improves Cancer therapy. *J. Controlled Release* **2014**, *183*, 18−26.
(133) Chen, B.; van der Poll, D. G.; Jerger, K.; Floyd, W. C.; Fréchet, J. M. J.; Szoka, F. C. Synthesis and Properties of Star-Comb Polymers and Their Doxorubicin Conjugates. *Bioconjugate Chem.* **2011**, *22*, 617−624.
(134) Zanini, D.; Park, W. K. C.; Roy, R. Synthesis of Novel Dendritic Glycosides. *Tetrahedron Lett.* **1995**, *36*, 7383−7386.
(135) Ashton, P. R.; Boyd, S. E.; Brown, C. L.; Nepogodiev, S. A.; Meijer, E. W.; Peerlings, H. W. I.; Stoddart, J. F. Synthesis of Glycodendrimers by Modification of Poly(propylene imine) Dendrimers. *Chem.—Eur. J.* **1997**, *3*, 974−984.
(136) André, S.; Pieters, R. J.; Vrasidas, I.; Kaltner, H.; Kuwabara, I.; Liu, F.-T.; Liskamp, R. M. J.; Gabius, H.-J. Wedgelike Glycodendrimers as Inhibitors of Binding of Mammalian Galectins to Glycoproteins, Lactose Maxiclusters, and Cell Surface Glycoconjugates. *ChemBioChem.* **2001**, *2*, 822−830.
(137) Ladmiral, V.; Melia, E.; Haddleton, D. M. Synthetic Glycopolymers: An Overview. *Eur. Polym. J.* **2004**, *40*, 431−449.
(138) Okada, M. Molecular Design and Syntheses of Glycopolymers. *Prog. Polym. Sci.* **2001**, *26*, 67−104.
(139) Lundquist, J. J.; Toone, E. J. The Cluster Glycoside Effect. *Chem. Rev.* **2002**, *102*, 555−578.
(140) Fraser, C.; Grubbs, R. H. Synthesis of Glycopolymers of Controlled Molecular Weight by Ring-Opening Metathesis Polymerization Using Well-Defined Functional Group Tolerant Ruthenium Carbene Catalysts. *Macromolecules* **1995**, *28*, 7248−7255.
(141) Ejaz, M.; Ohno, K.; Tsujii, Y.; Fukuda, T. Controlled Grafting of a Well-Defined Glycopolymer on a Solid Surface by Surface-Initiated Atom Transfer Radical Polymerization. *Macromolecules* **2000**, *33*, 2870−2874.
(142) Peterson, J.; Allikmaa, V.; Subbi, J.; Pehk, T.; Lopp, M. Structural Deviations in Poly(amidoamine) Dendrimers: A MALDI-TOF MS Analysis. *Eur. Polym. J.* **2003**, *39*, 33−42.
(143) Shi, X.; Bányai, I.; Islam, M. T.; Lesniak, W.; Davis, D. Z.; Baker, J. R.; Balogh, L. P. Generational, Skeletal and Substitutional Diversities in Generation One Poly(amidoamine) Dendrimers. *Polymer.* **2005**, *46*, 3022−3034.
(144) Fei, X.; Gu, Y.; Lan, Y.; Shi, B. Fluorescent Properties of Novel Dendrimer Dyes Based on Thiazole Orange. *J. Lumin.* **2011**, *131*, 2148−2152.
(145) Mecke, A.; Lee, I.; Baker, J. R., Jr.; Holl, M. M.; Orr, B. G. Deformability of Poly(amidoamine) Dendrimers. *Eur. Phys. J. E* **2004**, *14*, 7−16.
(146) Minard-Basquin, C.; Weil, T.; Hohner, A.; Rädler, J. O.; Müllen, K. A Polyphenylene Dendrimer−Detergent Complex as a Highly Fluorescent Probe for Bioassays. *J. Am. Chem. Soc.* **2003**, *125*, 5832−5838.
(147) Xu, Z.; He, B.; Shen, J.; Yang, W.; Yin, M. Fluorescent Water-Soluble Perylenediimide-Cored Cationic Dendrimers: Synthesis, Optical Properties, And Cell Uptake. *Chem. Commun.* **2013**, *49*, 3646−3648.
(148) Zill, A. T.; Licha, K.; Haag, R.; Zimmerman, S. C. Synthesis and Properties of Fluorescent Dyes Conjugated to Hyperbranched Polyglycerols. *New J. Chem.* **2012**, *36*, 419−427.
(149) Al-Jamal, K. T.; Ruenraroengsak, P.; Hartell, N.; Florence, A. T. An Intrinsically Fluorescent Dendrimer as a Nanoprobe of Cell Transport. *J. Drug Targeting* **2006**, *14*, 405−412.
(150) Scheibe, C.; Wedepohl, S.; Riese, S. B.; Dernedde, J.; Seitz, O. Carbohydrate−PNA and Aptamer−PNA Conjugates for the Spatial Screening of Lectins and Lectin Assemblies. *ChemBioChem* **2013**, *14*, 236−250.
(151) Ornelas, C. t.; Pennell, R.; Liebes, L. F.; Weck, M. Construction of a Well-Defined Multifunctional Dendrimer for Theranostics. *Org. Lett.* **2011**, *13*, 976−979.
(152) Lim, J.; Simanek, E. E. Triazine Dendrimers as Drug Delivery Systems: From Synthesis to Therapy. *Adv. Drug Delivery Rev.* **2012**, *64*, 826−835.
(153) Simanek, E. E.; Abdou, H.; Lalwani, S.; Lim, J.; Mintzer, M.; Venditto, V. J.; Vittur, B. The 8 Year Thicket of Triazine Dendrimers: Strategies, Targets and Applications. *Proc. R. Soc. London, Ser. A* **2010**, *466*, 1445−1468.
(154) Lee, C.; Lo, S.-T.; Lim, J.; da Costa, V. C. P.; Ramezani, S.; Öz, O. K.; Pavan, G. M.; Annunziata, O.; Sun, X.; Simanek, E. E. Design, Synthesis and Biological Assessment of a Triazine Dendrimer with Approximately 16 Paclitaxel Groups and 8 PEG Groups. *Mol. Pharmaceutics* **2013**, *10*, 4452−4461.